J Sci Comput (2017) 71:274–302
DOI 10.1007/s10915-016-0299-1

A Locally Gradient-Preserving Reinitialization for Level Set Functions

Lei Li[1] · **Xiaoqian Xu**[2] · **Saverio E. Spagnolie**[2]

Received: 29 June 2016 / Revised: 6 September 2016 / Accepted: 23 September 2016 /
Published online: 5 October 2016

Abstract The level set method commonly requires a reinitialization of the level set function due to interface motion and deformation. We extend the traditional technique for reinitializing the level set function to a method that preserves the interface gradient. The gradient of the level set function represents the stretching of the interface, which is of critical importance in many physical applications. The proposed locally gradient-preserving reinitialization (LGPR) method involves the solution of three PDEs of Hamilton–Jacobi type in succession; first the signed distance function is found using a traditional reinitialization technique, then the interface gradient is extended into the domain by a transport equation, and finally the new level set function is found by solving a generalized reinitialization equation. We prove the well-posedness of the Hamilton–Jacobi equations, with possibly discontinuous Hamiltonians, and propose numerical schemes for their solutions. A subcell resolution technique is used in the numerical solution of the transport equation to extend data away from the interface directly with high accuracy. The reinitialization technique is computationally inexpensive if the PDEs are solved only in a small band surrounding the interface. As an important application, we show how the LGPR procedure can be used to make possible the local level set approach to the Eulerian Immersed boundary method.

Keywords Level-set method · Eulerian immersed boundary method · Fluid–structure interaction · Reinitialization

✉ Saverio E. Spagnolie
spagnolie@math.wisc.edu

Lei Li
leili@math.duke.edu

Xiaoqian Xu
xxu@math.wisc.edu

[1] Department of Mathematics, Duke University, Durham, NC 27708, USA

[2] Department of Mathematics, University of Wisconsin-Madison, Madison, WI 53706, USA

1 Introduction

The level set method [34,35] is a classical framework used to accurately and elegantly evolve Lagrangian interfaces over a fixed Eulerian grid. It has seen very wide application in numerous fields, from fluid–structure interactions (e.g., lipid vesicles [40], bubbles [5], two-phase flows [47]) to image processing [29], computational geometry [42], computer vision [42], and materials science [26,42]. The level set method involves the tracking of a level set function ϕ, a continuous function with the property that its zero level set $\Gamma = \{x : \phi(x) = 0\}$ represents the Lagrangian interface (e.g., the boundary between two fluid phases or an immersed elastic structure). However, if the interface is deformed by a velocity field, for instance, then the gradient of the associated level set function, $\nabla\phi$, may become unbounded in the process. To reduce the associated numerical error the level set function is commonly reinitialized. Even if the boundary is not highly deformed, when a local level set method [1,38] is applied to reduce computational costs, reinitialization is required if the interface approaches the boundary of the thin computational tube.

For many applications, only the position and curvature of the interface are needed, and the level set function ϕ after each reinitialization may be chosen to be a signed distance function [5,29,47]. For example, in the simulation of elastic structures immersed in a fluid, if the tension is assumed to be constant then the force depends only on the curvature of the interface and the signed distance function contains sufficient information [5]. However, in the Eulerian immersed boundary method [9,10], $|\nabla\phi|_\Gamma$ represents the stretching of the elastic structure. Consequently, the elastic forces depend on $|\nabla\phi|$ at the interface and the signed distance function cannot be used to compute these forces. One solution to this problem, shown by Cottet and Maitre [10], is to avoid reinitialization altogether and to instead renormalize with a particular approximation of the Dirac delta function used in interface capture. However, this strategy is unhelpful in some settings, for instance in the local level set approach to the Eulerian immersed boundary method when the interface approaches the edge of the computational tube and reinitialization is unavoidable.

In this paper we develop a method for reinitializing the level set function that locally preserves its gradient near the Lagrangian interface. The proposed locally gradient-preserving reinitialization (LGPR) method involves the solution of three Hamilton–Jacobi equations in succession; first the signed distance function is found using the traditional reinitialization technique, then the cost function is obtained by extending the interface gradient into the domain by a transport equation, and finally the new level set function is found by solving a generalized reinitialization equation with the cost function obtained in the previous step. The steady reinitialization equation is an eikonal equation with a cost function which is discontinuous at the cut locus of the interface. We prove that the "proper" viscosity solution (to be defined) of the eikonal equation with our particular discontinuous cost function exists and is unique, which is the desired level set function. The viscosity solution that vanishes at the interface of the reinitialization equation converges to this proper viscosity solution. Modification and combination of existing numerical schemes are proposed for the fast and accurate solution of the sequence of PDEs. As an important application, the LGPR technique makes the local level set approach to the Eulerian immersed boundary method possible, which may result in simulations comparable in cost with the classical immersed boundary method of Peskin [39] but with improved stability.

The paper is organized as follows. In Sect. 2 we present the sequence of PDEs involved in locally gradient-preserving reinitialization. In Sect. 3 we provide the theoretical results and give explicit formulas for viscosity solutions. Numerical schemes for solving the equations

are the topic of Sect. 4, and the procedure is used in a local level set approach to the Eulerian immersed boundary method in Sect. 5. A few illustrative examples are provided in Sect. 6. We conclude with a brief summary in Sect. 7. Proofs for several claims made throughout the paper about the cut locus, existence and uniqueness of the proper viscosity solution of the eikonal equation with a discontinuous cost function, and other issues are included in the Appendix.

2 Problem Setup and Reinitialization Method

We begin by describing in more detail the motivation and setup of the problem, and presenting the locally gradient-preserving reinitialization method. For the sake of presentation, we will consider as a model problem a closed one-dimensional elastic interface embedded in $\mathbb{R}^2$, though the method could be extended into cases with several closed interfaces or higher dimensions without conceptual difficulty.

Suppose ϕ is a level set function such that the zero level set Γ agrees with the interface $X(\xi, t)$, where ξ is a Lagrange coordinate and t is time. Assume that $\phi > 0$ inside Γ and $\phi < 0$ outside Γ. In [9], it was shown that $|\nabla\phi(X(\xi,t),t)|/|X_\xi(\xi,t)| = \alpha(\xi)$ is independent of t when ϕ is convected by the velocity field, and thus if ϕ is constructed initially such that $\alpha = 1$, $|\nabla\phi|_\Gamma$ measures the tangential stretching (or compression) of the interface. Generically, such an elastic structure responds energetically to both bending and stretching deformations. The elastic force due to interface bending depends on the curvature $\kappa = -\nabla\cdot\hat{n}$, where $\hat{n} = \nabla\phi/|\nabla\phi|$ is the inward-pointing normal vector at the interface, which is unchanged under any reinitialization scheme that preserves the location of the level set. The elastic force due to interface stretching, however, at a point x is given by:

$$\begin{aligned} F(x) &= \nabla\left(E'(|\nabla\phi|)\right)|\nabla\phi|\delta(\phi) - \nabla\cdot\left(E'(|\nabla\phi|)\frac{\nabla\phi}{|\nabla\phi|}\right)\nabla\phi\,\delta(\phi) \\ &= \kappa\,E'(|\nabla\phi|)\nabla\phi\,\delta(\phi) + E''(|\nabla\phi|)\hat{n}\cdot\nabla\nabla\phi\cdot(I-\hat{n}\hat{n})|\nabla\phi|\delta(\phi) \end{aligned} \tag{1}$$

(see [9]), where I is the identity operator, $\hat{n}\hat{n}$ is a dyadic product and $E(\cdot)$ is the elastic energy due to stretching. The first term in (1) is a force due to a curved interface under a certain tension, while the second term is due to tension gradients along the interface. We introduce the stretch function

$$\chi(x) = |\nabla\phi|(x), \quad x \in \Gamma \tag{2}$$

defined on the interface (time dependence is ignored). Stretching occurs in regions where $\chi > 1$, and compression occurs where $\chi < 1$. In the above, we require two quantities that may be tied to the gradient of the level set function: $\chi(x)$ and $\hat{n}\cdot\nabla\nabla\phi\cdot(I-\hat{n}\hat{n})|_\Gamma = D_s\chi(\Gamma(s))\hat{s}$, where s is the arc length parameter, $D_s = d/ds$ and $\hat{s} = \Gamma'(s)$ is the unit tangent vector along the surface Γ.

In the process of convecting the interface, $\nabla\phi$ may become unbounded (usually away from the interface), or the zero level set may drift towards the boundary of a tube in the local level set method. In this situation it is necessary to find a new level set function that is better behaved. In order to leave the elastic forces unchanged during this process, the stretch function χ must be preserved during reinitialization. In theory preserving $\chi(\Gamma(s))$ is sufficient, but in numerical application we must also ensure that its tangential derivative is accurately preserved. We now formulate the reinitialization problem in a more mathematical way.

2.1 Locally Gradient-Preserving Reinitialization

Suppose that ϕ_0 is a uniformly continuous level set function, C^1 on $\Gamma = \{x : \phi_0(x) = 0\}$ with $x \in \mathbb{R}^2$, but not necessarily C^1 elsewhere. ϕ_0 is assumed to be positive inside the interface Γ and negative outside Γ. In addition we assume that Γ satisfies:

Assumption 1 Γ is a closed, nonintersecting C^1 curve which can be decomposed into several segments, each of which is locally analytical throughout (including at the segment endpoints).

Consider an arc-length parameterization of the interface on one such segment, $\Gamma(s) : [a, b] \to \mathbb{R}^2$. Γ is locally analytical if for every $s_0 \in [a, b]$, there is a number $\varepsilon > 0$, so that the Taylor series of Γ about s_0 converges to Γ in $(s_0 - \varepsilon, s_0 + \varepsilon) \cap [a, b]$. That the segment endpoints are also assumed to be analytical (one-sided) removes certain pathological behaviors [6]. The assumption on Γ makes physical sense for practical interfaces.

We denote by U the open domain enclosed by Γ. The stretch function

$$\chi(x) = |\nabla\phi_0|(x), \quad x \in \Gamma \tag{3}$$

is assumed to satisfy: $\chi(\Gamma(s))$ is continuous and the derivative $D_s\chi(\Gamma(s))$ is piecewise continuous. We assume $0 < c_1 \le \chi(\Gamma(s)) \le c_2$ for two constants c_1, c_2, which is a physically relevant constraint since the stretching deformation is generally bounded when the material is elastic. We aim to find a new level set function ϕ which is Lipschitz continuous (the gradient is bounded), smooth (C^1) in a local band around Γ, and in particular, preserves the interface gradient, $|\nabla\phi|(x \in \Gamma) = \chi(x \in \Gamma)$.

We are then led to the eikonal equation,

$$\begin{aligned} H(x, \nabla\phi) = \operatorname{sgn}(\phi_0)(|\nabla\phi| - f(x)) = 0 \quad x \in \mathbb{R}^2, \\ \phi(x) = 0, \ x \in \Gamma, \end{aligned} \tag{4}$$

for some suitable f that has the boundary condition $f(x) = \chi(x)$ for $x \in \Gamma$. Here $H(x, p) = \operatorname{sgn}(\phi_0(x))(|p| - f(x))$ is the Hamiltonian. The sign function $\operatorname{sgn}(\phi_0)$ connects the level set function to the so-called viscosity solution, as will be discussed in the next section. While f is known on Γ, part of the reinitialization process will be first to extend f away from the interface and into the larger domain.

In the traditional reinitialization procedure, the new level set function φ is the signed distance function which is recovered by solving numerically a Hamilton–Jacobi (H–J) equation [47],

$$\begin{aligned} \frac{\partial\varphi}{\partial\tau} + \operatorname{sgn}(\phi_0)(|\nabla\varphi| - 1) = 0, \\ \varphi(x, 0) = \phi_0(x), \end{aligned} \tag{5}$$

which is inadequate in our effort to preserve the interface stretch information.

Instead, we propose continuing the process by two extra steps to find a new function ϕ that shares its gradient with ϕ_0 locally near Γ. First, we extend $f(x \in \Gamma) = \chi(x \in \Gamma)$ from the interface out into the whole domain along the characteristic lines of the signed distance function by a transport equation,

$$\begin{aligned} \frac{\partial f}{\partial\tau} + \operatorname{sgn}(\varphi)\nabla\varphi \cdot \nabla f = 0, \\ f(x \in \Gamma, \tau) = \chi(x). \end{aligned} \tag{6}$$

The desired level set function is then obtained by solving a generalized reinitialization equation,

$$\begin{aligned} &\frac{\partial \phi}{\partial \tau} + \operatorname{sgn}(\phi_0)(|\nabla \phi| - f(x)) = 0, \\ &\phi(x, 0) = \phi_0(x). \end{aligned} \tag{7}$$

For the remainder of the paper, references to the "reinitialization equation" are to (7); the earlier equation (5), a special case of (7), will be referred to as the traditional reinitialization equation. For convenience we have abused the notation for $f(x, \tau)$ and the steady cost function $f(x)$, and similarly $\phi(x, \tau)$ and ϕ. Whether we mean the steady solution or the pseudo-time dependent solution should be clear by the context. We refer to (5)–(7) as the locally gradient-preserving reinitialization (LGPR) method.

The LGPR method is straight-forward and there are no immediately apparent complications, but it is not obvious that the solution of (7) converges to the solution of the eikonal equation (4), or even if it exists since the cost function f developed with the transport equation in (6) may be discontinuous. However, as we will show in the following section, the solutions so obtained are well-defined so that the reinitialization method presented here may become a basis for fast, accurate local level set methods. We will also numerically determine how to preserve the interface gradient χ so that $D_s \chi(\Gamma(s))$ can be recovered accurately.

Remark 1 When $f(x)$ is known in the whole domain, the eikonal equation, Eq. (4) can be solved using, for instance, the fast marching method (FMM) [41] or the fast sweeping method (FSM) [52]. This is one approach for initializing an original level set function, and could also be used as an alternative basis for reinitialization.

3 Theoretical Results

In this section we will show that the LGPR equations described in the previous section are well-posed. Specifically, we will show that the cost function $f(x)$ is continuous outside of a closed set consisting of arcs and vertices and that the eikonal equation has a unique "proper" solution (to be clarified later) given the function $f(x)$ produced using the transport equation (6). A formula for $\phi(x, \tau)$ is derived, which is found to converge to the "proper" solution of the eikonal equation (4) in finite time on any bounded set. Thus, (7) is shown to be equivalent to (4).

While the eikonal equation and Hamilton–Jacobi equations with discontinuous Hamiltonians have been studied by numerous authors [14,16,37,43–45], the results available in the literature do not apply to our particular equations (For the details, see Appendix B). Namely, in the references just cited, assumptions are made that do not apply to the cost function generated by (6). Meanwhile, the equation $u_t + \operatorname{sgn}(u_0) H(\nabla u) = 0$ has been studied in [2] but (7) does not belong to this class. In our theoretical results, the proof of uniqueness for our particular eikonal equation is new, and the formula for $\phi(x, \tau)$ is, to the best of our knowledge, derived for the first time.

3.1 The Eikonal Equation

The eikonal equation (4), is a Hamilton–Jacobi equation with Hamiltonian $H(x, p) = \operatorname{sgn}(\phi_0(x))(|p| - f(x))$, and f is called the cost function. We first introduce the definition of viscosity solutions (see [12,19]), then we study the continuity (and regions of discontinuity)

of f from its development by (6), and finally explore the associated solutions of the eikonal equation.

3.1.1 Viscosity Solutions of the Eikonal Equation

In the general setting of the eikonal equation, solutions need not exist in the classical sense. Instead, solutions are developed in a weaker sense; specifically, a viscosity solution is defined as follows.

Definition 1 A viscosity sub-solution (super-solution) of $H(x, \nabla\phi) = 0$ is an upper semi-continuous function (a lower semi-continuous function), if for any C^∞ function ζ, when $\phi - \zeta$ has a local maximum (minimum) at x_0 which is an interior point, then $H_*(x_0, \nabla\zeta(x_0)) \leq 0$ $(H^*(x_0, \nabla\zeta(x_0)) \geq 0)$. A viscosity solution is a continuous function that is both a sub- and super-solution.

In this definition, $H^*(x, p) = \lim_{r\to 0} \text{esssup}\{H(y, q) |\ \|(y, q) - (x, p)\|_{L^2} \leq r\}$ is the sup-envelope, and H_* is similarly defined to be the inf-envelope.

For example, consider $|u'| = 1, x \in (-1, 1)$ with $\Gamma = \{-1, 1\}$ (see exercises in [15]) whose viscosity solution is $u = 1 - |x|$ for $x \in [-1, 1]$. The viscosity solution of $-|u'| = -1, x \in (-1, 1)$ with $\Gamma = \{-1, 1\}$ is $u = |x| - 1$ for $x \in [-1, 1]$. From this definition, we see why $\text{sgn}(\phi_0)$ appears in the eikonal equation: the viscosity solution of $|\nabla\phi| - f = 0$ can only have kinks pointing up while the viscosity solution of $f - |\nabla\phi| = 0$ can only have kinks pointing down. If we write the eikonal equation as $|\nabla\phi| = f$, for Γ that is not convex, ϕ that is negative outside Γ may have kinks pointing down and this ϕ is not a viscosity solution to $|\nabla\phi| = f$. A common error in the numerical literature is that the signed distance function associated with a non-convex curve is treated as a viscosity solution of $|\nabla\phi| = 1$.

It is natural to decompose the eikonal equation (4), into interior $(x \in U)$ and exterior $(x \in \mathbb{R}^2 \setminus \bar{U})$ problems, and to piece the two solutions together. If f is continuous at Γ, which it is as we will show, then the interior and exterior solutions together form a viscosity solution over the entire domain (since the equation is also then satisfied on the interface Γ). We therefore focus on the interior and exterior problems separately.

The interior problem has been solved by other authors for continuous f with $\inf f > 0$, and existence and uniqueness have been established [12,21,24]. An integral representation of ϕ is given by:

$$\phi(x) = \inf_{\gamma\in\mathscr{C}} \left\{ \int_0^L f(\gamma(s))ds \,\middle|\, \gamma(0) = x, \quad \gamma(L) \in \Gamma \right\}, \tag{8}$$

(see [28,37]), where $\mathscr{C}$ is the class of absolutely continuous self-avoiding curves, s is the arc-length parameter, and L is the total arc-length (which depends on γ).

In the exterior problem, however, even if f is continuous and $\inf f > 0$, uniqueness is not guaranteed. For example, both $\phi_1(x) = ||x| - 1|$ and $\phi_2(x) = 1 - |x|$ where $x \in \mathbb{R}$ are viscosity solutions for $\text{sgn}(1 - |x|)(|\phi'(x)| - 1) = 0$. This motivates the following definition:

Definition 2 The "proper" viscosity solution of the eikonal equation (4), is defined to be the pointwise limit of ϕ_n as $n \to \infty$, where ϕ_n is the viscosity solution satisfying (4) in the sense of Definition 1 in $\{|x| < n\}$ with $\phi_n(|x| = n) = 0$ for $n \in \mathbb{Z}$ and $n > \max_{y\in\Gamma} d(0, y)$.

Here $d(E_1, E_2) = \inf_{x\in E_1, y\in E_2} \|x - y\|$ is the distance between two sets E_1 and E_2. Under this definition, for continuous $f > 0$, ϕ is the limit of a sequence of interior problems and is therefore uniquely determined (see the previous discussion). Such a ϕ is also a viscosity solution in the general sense of Definition 1. A limit of the integral representation of ϕ_n as $n \to \infty$ reveals the viscosity solution for all $x \in \mathbb{R}^2$ with continuous $f > 0$, so that a representation of $\phi(x)$ for all x is given by

$$\phi(x) = \text{sgn}(\phi_0) \inf_{\gamma\in\mathscr{C}} \left\{ \int_0^L f(\gamma(s))ds \,\middle|\, \gamma(0) = x, \quad \gamma(L) \in \Gamma \right\}. \tag{9}$$

Unfortunately, while continuous on Γ, it is not guaranteed that the f obtained by the transport equation (6), is continuous in the whole domain. Before proceeding any further, we must therefore understand the nature of f obtained using (6).

3.1.2 The Cost Function

Due to the method for extending f into the whole domain using (6), the behavior of the cost function f is intimately linked to the behavior of φ. Aujol and Aubert [2] have shown that the viscosity solution of (5) that satisfies $\varphi(x \in \Gamma, \tau) = 0$ converges to the steady solution, which is the proper viscosity solution (see Definition 2) of $\text{sgn}(\phi_0)(|\nabla\varphi| - 1) = 0$. By (9), since the cost function in this case is 1, φ is the signed distance function:

$$\varphi(x) = \begin{cases} d(x, \Gamma) & x \in \bar{U}, \\ -d(x, \Gamma) & x \in \mathbb{R}^2 \setminus \bar{U}. \end{cases} \tag{10}$$

φ is therefore 1-Lipschitz continuous, and hence differentiable almost everywhere (a.e.). Of particular importance is the singular set of φ, which is most conveniently uncovered by studying a projection to the interface:

Definition 3 $Px = \{y \in \Gamma | d(x, \Gamma) = d(x, y)\}$ is the nonempty projection of x onto Γ. Let $A = \{x | \#Px \geq 2\}$ be the set of points for which the distance is achieved at multiple boundary points. The part of A inside of Γ is called the medial axis, and its closure $\bar{A}$ is called the cut locus. The skeleton S is the set of centers of maximal circles (with order defined by inclusion) inside Γ.

First note that by the C^1 assumption on Γ we have that the distance between the cut locus and the interface is always positive, $d(\bar{A}, \Gamma) > 0$. For $x \notin \bar{A} \cup \Gamma$, we have that

$$\nabla d(x, Px) = \frac{x - Px}{|x - Px|}, \tag{11}$$

since Px and $d(x, Px)$ are both differentiable at such a point, and since $P(tx + (1-t)Px) = Px$ for $0 < t < 1$. Therefore, $\nabla\varphi = \text{sgn}(\phi_0)\nabla d(x, Px)$ is continuously extended to Γ, and thus φ is C^1 at Γ. Moreover, the line $x - Px$ is a characteristic line of φ due to its alignment with ∇d. Therefore, f is constant along the line $x - Px$ by (6); in addition, $f(x, \tau)$ is steady when $\tau > d(x, \Gamma)$ and $f(x) = \chi(Px)$. f is continuous at x since Px is. f is thus continuous for all $x \notin \bar{A}$ and is given by $f(x) = \chi(Px)$.

Having shown f to be continuous everywhere outside of the cut locus, we are left now to explore $x \in \bar{A}$. It is well known that $\varphi(x) = \text{sgn}(\phi_0)d(x, Px)$ is not differentiable at any point in A, but due to the importance of the result for studying our method, we provide an alternative proof in Appendix A for reference. Also note that $A \cap U \subset S \subset \bar{A} \cap U$ [27]. By the assumptions on Γ, the curvature κ of Γ exists except at possibly a finite number of points,

and even at these points the left and right limits of the curvature exist; thus $\sup|\kappa| < \infty$. When U is convex, this provides an estimate for the distance between the cut locus and the interface: $d(\bar{A}, \Gamma) \geq \inf\{1/\kappa\}$ (see Appendix A; the chosen convention is that the curvature of a circle is positive). In general, however, there is no estimate for $d(\bar{A}, \Gamma)$. To proceed, we must further investigate the structure of the cut locus $\bar{A}$. To this end, we observe the following:

Lemma 1 *Let $x \in \mathbb{R}^2$. For any $y \in Px$, let $z(t) = ty + (1-t)x$, $0 < t \leq 1$. Then, $Pz(t) = \{y\}$ and $z(t) \notin \bar{A}$.*

Proof The only nontrivial part of this claim is that $z(t) \notin \bar{A} \setminus A$. Suppose $z(t) \in \bar{A} \setminus A$ for some t. Then $z(t)$ is the center of the osculating circle of Γ at y, and the circle centered at x with radius $d(x, y)$ contains strictly a part of Γ inside, contradicting the fact that $y \in Px$. □

Remark 2 Based on this lemma and the assumptions on the boundary curve, we are able to see another interesting geometric property of the set $\bar{A}$: there are no cusps in $\bar{A}$ with zero angles (proved in Appendix A).

From Lemma 1, we have that the points in $\bar{A}$ are the terminal points of propagation along the characteristic lines of φ. Since the characteristics of φ meet at the cut locus, f may not be well defined there, so we define

$$f(x) = \inf_{y \in Px} \chi(y), \quad x \in \bar{A}. \tag{12}$$

Here notice f is extended to both the interior and exterior of the interface, which means we need to discuss the points both inside and outside of Γ. We first concentrate on points inside of Γ. From Theorem 6.2 and Corollary 7.1 of [6], we have that $\bar{S} = \bar{A} \cap U$ is simply connected and the union of finitely many points and finitely many locally analytical open curves. Moreover, for every point on these locally analytical curves, it has a projection of size exactly two.

Now consider $\bar{A}$ outside of Γ. Suppose U is convex, then $\bar{A} \cap U^c = \emptyset$. Otherwise, $\bar{A} \cap U^c$ may contain curves extending to infinity in general. Defining $U_n = B_n \cap \bar{U}^c$ with $B_n = \{|x| < n\}$, by the definition of the skeleton, the closure of the skeleton S_n of U_n agrees with the skeleton of $\bar{A} \cap U^c$ inside, for instance, $B_{n/3}$. This means for the points outside of Γ but inside of any bounded domain, by the result in [6] we also have a similar characterization as for the points inside of Γ (except the simple connectivity). To summarize, we have

Lemma 2 *The set $\bar{A} \cap U$ is simply connected, consisting of finitely many points and open curves where the curves are locally analytical and every point on those curves has a projection of size two. Meanwhile, in any bounded domain the set $\bar{A} \cap U^c$ consists of finitely many points and open curves that are locally analytical, and every point on those curves also has a projection of size two.*

For a point in $\bar{A}$ with a projection of size two, the function f defined in (12) has limiting values from both sides of the curve (proved in Appendix B). We now have the following theorem, which will be important in investigating existence and uniqueness of the viscosity solutions to the eikonal equation and the reinitialization equation:

Theorem 1 *The function f in (12) is bounded by c_1 and c_2 (Recall $c_1 \leq \chi(x \in \Gamma) \leq c_2$) and is continuous outside the cut locus (in $\mathbb{R}^2 \setminus \bar{A}$), and the cut locus is well-separated from the interface, $d(\bar{A}, \Gamma) > 0$. Except at finitely many points, f has a limit when x approaches $\bar{A}$ from one side of $\bar{A}$.*

3.1.3 Viscosity Solutions with a Discontinuous Cost Function

We may now investigate the solution of the eikonal equation when the cost function f is discontinuous with properties described in Theorem 1. The solution is the steady solution of the reinitialization equation and is hence the desired level set function. Existence has been proven in fact for a much broader class of cost functions [14]. Uniqueness, however, is more challenging. Uniqueness of the eikonal equation has been shown for cost functions f satisfying certain conditions not applicable to the present case [14,16,37,43–45], so we must develop uniqueness of the solution particular to the cost function f of the form in Theorem 1.

To begin, since f is continuous on Γ, we can split (4) into interior and exterior problems, as discussed in Sect. 3.1.1. We first consider the interior problem,

$$\begin{aligned} |\nabla\phi| - f(x) &= 0, \quad \text{if } x \in U, \\ \phi(x \in \Gamma) &= 0. \end{aligned} \tag{13}$$

We have here that $H_*(x,p) = (|p| - f)_* = |p| - f^*$ and $H^*(x,p) = (|p| - f)^* = |p| - f_*$, where the sup- and inf- envelopes were defined in Sect. 3.1.1. By Theorem 1, $0 < c_1 \le f^*, f_* \le c_2$. f^* is upper semi-continuous (USC) and f_* is lower semi-continuous (LSC). If f is continuous at x, $f^*(x) = f_*(x)$ and both f^*, f_* are continuous at x. By the way we define f in (12), we have $f = f_*$. It is simple to show if ϕ is differentiable at x_0, that $f_*(x_0) \le |\nabla\phi|(x_0) \le f^*(x_0)$ (see [15]). This implies that if ϕ is Lipschitz (thus differentiable a.e.), then $|\nabla\phi| = f$ outside a set of measure zero.

By approximating f by its sup- and inf-convolutions (see [14]):

$$f^\varepsilon(x) = \operatorname{esssup}_y\{f(y) - |y-x|^2/\varepsilon\}, \quad f_\varepsilon(x) = \operatorname{essinf}_y\{f(y) + |y-x|^2/\varepsilon\}, \tag{14}$$

two viscosity solutions of the eikonal equation (4) are found:

$$\phi_M(x) = \inf_{\gamma\in\mathscr{C}}\left\{\int_0^L f^*(\gamma(s))ds \,\middle|\, \gamma(0) = x, \quad \gamma(L) \in \Gamma\right\}, \tag{15}$$

$$\phi_m(x) = \inf_{\gamma\in\mathscr{C}}\left\{\int_0^L f_*(\gamma(s))ds \,\middle|\, \gamma(0) = x, \quad \gamma(L) \in \Gamma\right\}. \tag{16}$$

The detail of this proof of existence is routine [14], but for convenience it is provided in Appendix B. Note that f^* and f_* are integrable on every curve $\gamma \in \mathscr{C}$. Also in the Appendix, it is shown that ϕ_M and ϕ_m are Lipschitz continuous with the Lipschitz constant c_2. These two solutions are the maximal and minimal viscosity solutions of the eikonal equation [43–45]. The viscosity solution is unique if $\phi_M = \phi_m$. It is clear that $\phi_M = \phi_m$ if and only if for every point $x \in U$, there is a sequence of curves $\gamma_n \in \mathscr{C}$ with total length L_n (where $\gamma_n(0) = x$ and $\gamma_n(L_n) \in \Gamma$) such that

$$\phi_m(x) = \lim_{n\to\infty}\int_0^{L_n} f_*(\gamma_n(s))ds \quad \text{and} \quad \lim_{n\to\infty}\int_0^{L_n}(f^* - f_*)(\gamma_n(s))ds = 0. \tag{17}$$

The condition implies that $\phi_M(x) \le \phi_m(x)$; hence the two are equal. Conversely, if $\phi_M(x) = \phi_m(x)$, the condition is a straightforward corollary of the definition.

Uniqueness proofs in the literature do not apply to the discontinuous cost function f of Theorem 1. However, the uniqueness conditions (17) can be checked directly (see Appendix B for details). The proof of uniqueness in Appendix B is new and it can be modified to prove uniqueness of the eikonal equation for a broader class of discontinuous cost functions.

In the exterior problem, uniqueness of the proper viscosity solution may be proved by first considering the finite domain $\bar{U}^c \cap B_n$ with $B_n = \{|x| < n\}$, where ϕ_n satisfies $\phi_n(x) = 0$ at $|x| = n$, using a similar proof as in the interior problem and then taking $n \to \infty$. Recalling that $f = f_*$, we finally have the desired result:

Theorem 2 *The proper viscosity solution to* (4) *with the cost function obtained from* (6) *is unique and is given by* (9)*. It is hence c_2-Lipschitz continuous and C^1 in $\mathbb{R}^2 \setminus \bar{A}$.*

3.2 The Reinitialization Equation

Finally, we show that the reinitialization equation has viscosity solutions, and that the solution which is zero on Γ is unique and converges to the proper viscosity solution of the eikonal equation (4). Recall the reinitialization equation, written more generally as

$$\begin{aligned} &\frac{\partial u}{\partial \tau} + \operatorname{sgn}(u_0)(|\nabla u| - g(x)) = 0, \\ &u(x, 0) = u_0(x), \end{aligned} \tag{18}$$

where $u_0 \in UC(\mathbb{R}^2)$, with UC the class of uniformly continuous functions. Here u could be φ or ϕ and g could be 1 or f, and the Hamiltonian is written as $H(x, p) = \operatorname{sgn}(u_0(x))(|p| - g(x))$. We assume that $0 < c_1 \le g \le c_2$ and that Γ is the zero level set of u_0.

For time-dependent Hamilton–Jacobi equations, the classical solutions are not well-defined beyond the intersection of characteristics. For some applications, the multi-valued solutions are important [22]; for our purpose, we need the viscosity solution, whose definition is similar to the one for the eikonal equation in (1), with the only difference being the addition of a time derivative.

Generally, if g is not continuous, we can again approximate g by g^ε and g_ε and take the limit $\varepsilon \to 0$ as we did for the eikonal equation. Therefore, we first consider the case where g is continuous. Motivated by the solutions of the eikonal equation and the solution provided in [2] for $g = 1$, we construct the formula of the solution,

$$u(x, \tau) = \begin{cases} \operatorname{sgn}(u_0) \inf_{\gamma \in \mathscr{C}} \{|u_0(\gamma(\tau))| + \int_0^\tau g(s) ds \,|\, \gamma(0) = x\} & \tau \le \tau_x, \\ \operatorname{sgn}(u_0) \inf_{\gamma \in \mathscr{C}} \{\int_0^L g(s) ds \,|\, \gamma(0) = x, \gamma(L) \in \Gamma\} & \tau > \tau_x, \end{cases} \tag{19}$$

where τ_x is given by

$$\begin{aligned} \tau_x = \inf \Bigg\{ \bar{\tau} \ge d(x, \Gamma) \,\Big|\, \forall \tau > \bar{\tau} : \inf_{\gamma \in \mathscr{C}} \Big\{ |u_0(\gamma(\tau))| + \int_0^\tau g(s) ds \,\Big|\, \gamma(0) = x \Big\} \\ > \inf_{\gamma \in \mathscr{C}} \Big\{ \int_0^L g(s) ds \,\Big|\, \gamma(0) = x, \quad \gamma(L) \in \Gamma \Big\} \Bigg\}. \end{aligned} \tag{20}$$

It is evident that τ_x is continuous on x and $\tau_x \le c_2\, d(x, \Gamma)/c_1$. At τ_x the two expressions in (19) are equal. Otherwise, the first is always strictly larger than the second for all $\tau \ge d(x, \Gamma)$, but this cannot be true at $\tau = L_{opt} \ge d(x, \Gamma)$, where $L_{opt} = \liminf_{n \to \infty} L_n$ and L_n is a sequence such that $\exists \gamma_n, \gamma_n(0) = x, \gamma_n(L_n) \in \Gamma$, $\lim_{n \to \infty} \int_0^{L_n} g(\gamma_n(s)) ds = \inf_{\gamma \in \mathscr{C}} \int_0^L g(\gamma(s)) ds$. In addition, we find that $d(x, \Gamma) \le L_{opt} \le \tau_x \le c_2 d(x, \Gamma)/c_1$.

Remark 3 If one were to define a simpler time,

$$\tau_x = \inf\left\{\tau \Big| \inf_{\gamma\in\mathscr{C}}\left\{|u_0(\gamma(\tau))| + \int_0^\tau g(s)ds \;\Big|\; \gamma(0) = x\right\}\right.$$
$$\left. > \inf_{\gamma\in\mathscr{C}}\left\{\int_0^L g(s)ds \;\Big|\; \gamma(0) = x, \quad \gamma(L) \in \Gamma\right\}\right\}, \tag{21}$$

then τ_x might be smaller than L_{opt}. When $u(x,\tau)$ is given by the second formula, there could be no paths with lengths less than $\tau + \varepsilon_n$, $\varepsilon_n \to 0$ to approximate the infimum. For τ bigger than so-defined τ_x, the first expression might be smaller than the second one. The dynamic programming principle in Appendix C then cannot be shown.

Remark 4 Equation (19) is reminiscent of the Lax–Hopf formula (see [15]). For Hamilton–Jacobi equations of the form $u_t + H(\nabla u) = 0$ and $u(x,0) = u_0(x)$ where $H(p)$ is convex and $H(p)/|p| \to \infty$ as $|p| \to \infty$, the Lax–Hopf formula reads:

$$u(x,t) = \inf\left\{\int_0^t L(\dot\gamma(s))ds + u_0(y) \;\Big|\; \gamma(0) = y, \gamma(t) = x\right\}$$
$$= \min_y\left\{tL\left(\frac{x-y}{t}\right) + u_0(y)\right\}, \tag{22}$$

where L is the Legendre transform of H. In the special case $g = 1$, for x inside Γ, $H(p) = |p| - 1$, with $L(z) = 1$ if $|z| \le 1$ and $L(z) = \infty$ if $|z| > 1$. If $t < \tau_x$, one can check that (19) is the same as the Lax–Hopf formula, though $(|p| - 1)/|p| \to \infty$ is not satisfied. In the present problem there is a boundary Γ, and for general $g = g(x)$ the Hamiltonian also depends on x, resulting in an expression which differs from the Lax–Hopf formula.

The two expressions given in (19) are continuous in both x and τ and they give the same value at $\tau = \tau_x$. u is then continuous in both x and τ. We can also see that it satisfies the initial and boundary conditions of the reinitialization equation. In Appendix C, we verify that u is a viscosity solution. From the formula, since τ_x is bounded by $c_2 d(x,\Gamma)/c_1$, we see that the solution on any compact set converges to the proper viscosity solution of the eikonal equation (9) in finite time.

Uniqueness of the solution may be shown under the assumption that $u(x \in \Gamma, \tau) = 0$, which can be ensured numerically. Following [2], consider

$$\begin{aligned} &\frac{\partial u}{\partial \tau} + (|\nabla u| - g) = 0 \quad x \in U, \\ &u(x,0) = u_0(x) \quad x \in \bar U \\ &u(x \in \Gamma, \tau) = 0, \end{aligned} \tag{23}$$

and

$$\begin{aligned} &\frac{\partial u}{\partial \tau} - (|\nabla u| - g) = 0 \quad x \in \mathbb{R}^2 \setminus \bar U, \\ &u(x,0) = u_0(x) \quad x \in \mathbb{R}^2 \setminus U \\ &u(x \in \Gamma, \tau) = 0. \end{aligned} \tag{24}$$

The uniqueness of the solutions for these two problems have been established if g is continuous and bounded below by a positive number [20]. This is enough to say that there is at most one viscosity solution satisfying $u(x \in \Gamma, \tau) = 0$. One common mistake in the literature is

to assume that, since $\text{sgn}(u_0(x \in \Gamma)) = 0$, that $u_\tau(x \in \Gamma) = 0$ by (18). However, this argument is inadequate in the viscosity sense, since the set of viscosity solutions are unchanged by a redefinition of the sign function to a value $\text{sgn}(0) \in [-1, 1]$. It is sensible, however, that all viscosity solutions should have $u(x \in \Gamma, \tau) = 0$ as the characteristics flow out of Γ, and fortunately we can develop numerical schemes to ensure $u(x \in \Gamma, \tau) = 0$.

Finally, for g equal to the cost function f obtained from (6), it may be discontinuous as previously discussed. As was done for the eikonal equation, approximating f with f^ε and f_ε, and taking $\varepsilon \to 0$, we have the maximal and minimal solutions with g replaced by f^* and f_*. And as for the eikonal equation, these two are equal and the solution that is zero on the interface Γ is unique:

Theorem 3 *Assume in* (18) *that either* $g = 1$ *or* $g = f$ [*the cost function obtained using* (6)]. *The viscosity solution that satisfies* $u(x \in \Gamma) = 0$ *is unique and is provided in* (19). *This solution converges to the proper viscosity solution of* (4).

4 Numerical Schemes

We have shown in theory that the LGPR method yields the desired level set function. We proceed to describe numerical schemes for solving the PDEs introduced in Sect. 2 using classical methods with some modifications [30,38]. We also show how subcell resolution may be used to extend the interface gradient away from the surface with high accuracy. First we present a numerical scheme for solving the transport equation which involves a second-order accurate upwind Essentially Non-Oscillatory (ENO) scheme with subcell resolution in space and Gauss–Seidel iteration in time, and then we describe a method for solving the reinitialization equation which involves a Godunov numerical Hamiltonian scheme in space and again Gauss–Seidel iteration in time.

4.1 Numerical Setup

Consider a rectangular Eulerian grid with uniform grid spacing h upon which the interface Γ is overlaid. Gridpoints (x_i, y_j) are defined by $x_i = ih$ and $x_j = jh$, with i and j taking integer values. (Unlike in the theoretical part of the paper above, in which x and y correspond to two points in $\mathbb{R}^2$, in the remainder of the paper x and y are coordinates, $(x, y) \in \mathbb{R}^2$).

In order to approximate derivatives of possibly non-smooth functions we will rely on ENO finite differences (see [36]). In addition, in the solution of Hamilton–Jacobi equations, one-sided (upwind) derivatives are commonly used to retain causality (i.e. information follows the characteristics). In this paper, the following one-sided second order ENO finite differences will be used to approximate first derivatives,

$$\begin{aligned} D_x^- \phi_{i,j} &= \frac{\phi_{i,j} - \phi_{i-1,j}}{h} + \frac{h}{2}\text{minmod}(D_{xx}\phi_{i,j}, D_{xx}\phi_{i-1,j}), \\ D_x^+ \phi_{i,j} &= \frac{\phi_{i+1,j} - \phi_{i,j}}{h} - \frac{h}{2}\text{minmod}(D_{xx}\phi_{i,j}, D_{xx}\phi_{i+1,j}), \\ \text{minmod}\{a, b\} &= \begin{cases} 0 & \text{if } ab < 0, \\ \text{sgn}(a)\min\{|a|, |b|\} & \text{else,} \end{cases} \end{aligned} \tag{25}$$

where the second derivative is given by the centered difference formula

$$D_{xx}\phi_{i,j} = \frac{1}{h^2}\left(\phi_{i+1,j} - 2\phi_{i,j} + \phi_{i-1,j}\right). \tag{26}$$

4.2 The Transport Equation

Recall the definitions of the stretch function $\chi(x) = |\nabla\phi|(x)$ on $x \in \Gamma$ and the inward pointing unit normal vector $\hat{n} = \nabla\phi/|\nabla\phi|$. In solving the transport equation, we aim to accurately preserve the stretch function as well as its tangential derivative along the interface,

$$\hat{n} \cdot \nabla\nabla\phi \cdot (I - \hat{n}\hat{n})|_{\Gamma} = D_s \chi(\Gamma(s))\hat{s}, \tag{27}$$

where s is the arc-length and $\hat{s}(s) = \Gamma'(s)$ is the unit vector tangent to the surface Γ. Our strategy will be to preserve the zero level set of ϕ (the location of the surface Γ) and the stretch function χ with at least second order accuracy, and thus $D_s \chi(\Gamma(s))\hat{s}$ is formally preserved with first order accuracy.

In the solution of the transport equation we will use a subcell resolution (SR) technique to obtain the cost function f [see Eq. (4)]. In SR, the interface is determined by interpolating the obtained signed distance function φ, computing the the gradient there, and modifying the one-sided ENO derivatives according to the interface [18,30]. To illustrate the subcell resolution technique, consider as an example the case $\varphi_{ij}\varphi_{i-1,j} \le 0$. Letting

$$a_{ij} = h^2 \text{minmod}(D_{xx}\varphi_{ij}, D_{xx}\varphi_{i-1,j}), \tag{28}$$

and assuming $(x_\Gamma, y_j) \in \Gamma$, x_Γ is found by quadratic interpolation at $\varphi_{i-1,j}, \varphi_{ij}$ using the second order derivative a_{ij}/h^2. The approximations of the first derivatives are then given by

$$\begin{aligned} \partial_x \phi_0(x_\Gamma, y_j) &\approx \frac{\delta_{ij}^{x-}}{h} D_x^0 \phi_{0,i-1,j} + \frac{h - \delta_{ij}^{x-}}{h} D_x^0 \phi_{0,ij}, \\ \partial_y \phi_0(x_\Gamma, y_j) &\approx \frac{\delta_{ij}^{x-}}{h} D_y^0 \phi_{0,i-1,j} + \frac{h - \delta_{ij}^{x-}}{h} D_y^0 \phi_{0,ij}, \end{aligned} \tag{29}$$

where D_x^0, D_y^0 are the centered differences and

$$\delta_{ij}^{x-} = x_i - x_\Gamma = h\left(\frac{1}{2} + \frac{(\varphi_{ij} + \varphi_{i-1,j}) - a_{ij}/4}{(\varphi_{ij} - \varphi_{i-1,j}) + \text{sgn}(\varphi_{ij} - \varphi_{i-1,j})\sqrt{D_{ij}}}\right), \tag{30}$$

where

$$D_{ij} = (a_{ij}/2 - \varphi_{ij} - \varphi_{i-1,j})^2 - 4\varphi_{ij}\varphi_{i-1,j}. \tag{31}$$

Having now obtained the cost function on the interface, $f(x_\Gamma, y_j) = \sqrt{\partial_x \phi_0^2 + \partial_y \phi_0^2}$, the left ENO derivative of f at (i, j) is modified as

$$D_x^- f_{ij} = \frac{f_{ij} - f(x_\Gamma, y_j)}{\delta_{ij}^{x-}} + \frac{\delta_{ij}^{x-}}{2} \text{minmod}(D_{xx} f_{i-1,j}, D_{xx} f_{ij}),$$

while D_x^+ at $(i - 1, j)$ is similarly modified. To extend the quantities away from Γ, one approach is to compute the values at the grid points in a thin tube near the interface directly and then extend them out to other grid points using an upwind scheme. We instead use subcell resolution and completely avoid the tube, resulting in a simpler computation.

Next, the cost function f is extended into space by solving the transport equation,

$$\frac{\partial f}{\partial \tau} + \nabla d \cdot \nabla f = 0, \tag{32}$$

where $\nabla d = \text{sgn}(\varphi)\nabla\varphi$. We will denote $\text{sgn}(\varphi_{ij})D_x^{\pm}\varphi_{ij}$ by $D_x^{\pm}d_{ij}$ (where $D_x^{\pm}$ are acting on φ not $|\varphi|$ and $D_x^{\pm}$ are modified with subcell resolution near the interface) and we define

$$D_x d_{ij} = \text{maxabs}\{\max\{D_x^- d_{ij}, 0\},\ \min\{0, D_x^+ d_{ij}\}\}, \tag{33}$$

where $\text{maxabs}\{a, b\} = (a - b)\mathbb{1}_{\{|a|\geq|b|\}} + b$. For the numerical gradient we then take

$$\eta_{ij}^x = \frac{D_x d_{ij}}{\sqrt{(D_x d_{ij})^2 + (D_y d_{ij})^2 + \varepsilon^2}}, \quad \eta_{ij}^y = \frac{D_y d_{ij}}{\sqrt{(D_x d_{ij})^2 + (D_y d_{ij})^2 + \varepsilon^2}}, \tag{34}$$

where ε is a small parameter (chosen here to be 10^{-7}) to avoid the case that both D_x and D_y are close to zero at potentially irregular points. $D_x d_{ij}$ is so chosen to ensure that the information propagating to (i, j) is coming from points closer to the interface, which follows the correct characteristic directions, and also that any oscillation in f on the the cut locus $\bar{A}$ (see Definition 3), is suppressed. Using the definitions above, a complete spatial discretization for the transport equation is given by

$$L_T(f_{ij}) = -\left((\eta_{ij}^x)^+ D_x^- f_{ij} - (\eta_{ij}^x)^- D_x^+ f_{ij} + (\eta_{ij}^y)^+ D_y^- f_{ij} - (\eta_{ij}^y)^- D_y^+ f_{ij}\right), \tag{35}$$

where $a^+ = \max\{a, 0\}$ and $a^- = -\min\{a, 0\}$.

We now turn to the discretization of time, τ, which is not real time but merely a parameter used to relax the system to its steady state. Different timesteps k_{ij} are chosen for different points to ensure stability. Since $\delta_{ij}^{x\pm}$ or $\delta_{ij}^{y\pm}$ can be small, a Courant–Friedrichs–Lewy (CFL) condition for convergence requires that the time step be small near the interface. We use the same convention as in [30],

$$k_{ij} = C\min\{h, \delta_{ij}^{x\pm}, \delta_{ij}^{y\pm}\}, \tag{36}$$

where C is a constant taken small enough to ensure convergence. We choose $C = 1/2$ for the numerical examples to come, which is sufficient for the cases studied. Further, a Gauss–Seidel iteration is employed (values are updated using the newest data along the chosen sweeping directions) to allow information to propagate long distances in some directions with one iteration (see [52]). The Gauss–Seidel iteration is given by

$$f_{ij} \leftarrow f_{ij} + k_{ij} L_T(f_{ij}) \tag{37}$$

along the four sweeping directions $(i, j) = (1 : N, 1 : N)$, $(i, j) = (1 : N, N : -1 : 1)$, $(i, j) = (N : -1 : 1, 1 : N)$, and $(i, j) = (N : -1 : 1, N : -1 : 1)$, repeatedly.

Remark 5 For the application of a local level set method, it may be preferable to use a direct time-stepping method. One possibility is the second-order TVD Runge–Kutta method,

$$\begin{aligned} \tilde{f}_{ij}^{n+1} &= f_{ij}^n + k_{ij} L_T(f_{ij}^n), \\ f_{ij}^{n+1} &= \frac{1}{2}\left(f_{ij}^n + \tilde{f}_{ij}^{n+1}\right) + \frac{k_{ij}}{2} L_T\left(\tilde{f}_{ij}^{n+1}\right). \end{aligned} \tag{38}$$

Remark 6 For the transport equation (6), in many references $\nabla\varphi$ is discretized using a centered difference approximation. Near the interface, the signed distance function is C^1 so that this simple treatment is convenient and sufficient. However, once f is extended into the domain where the signed distance function is not smooth, the scheme developed in this section is expected to be more accurate.

The transport equation is solved using the standard upwind scheme, with improvements using ENO derivatives, subcell resolution and Gauss–Seidel sweeping (see [36,51]). While a rigorous proof which includes these improvements would be challenging, our numerical experiments suggest a natural convergence, and the limit outside the cut locus is indeed the cost function f.

4.3 The Reinitialization Equation

We now introduce the Godunov Hamiltonian scheme used to solve the reinitialization equation. By a similar consideration of causality, we use the Godunov Hamiltonian $\hat{H}_{ij}(D_x^- u_{ij}, D_x^+ u_{ij}, D_y^- u_{ij}, D_y^+ u_{ij})$, where $s_{ij} = \mathrm{sgn}(u_0(x_i, y_j))$, and

$$\hat{H}_{ij}(a,b,c,d) = \begin{cases} s_{ij}\left(\sqrt{\max\{a^+, b^-\}^2 + \max\{c^+, d^-\}^2} - g_{ij}\right) & \text{if } s_{ij} \geq 0, \\ s_{ij}\left(\sqrt{\max\{a^-, b^+\}^2 + \max\{c^-, d^+\}^2} - g_{ij}\right) & \text{if } s_{ij} < 0, \end{cases} \tag{39}$$

for spatial discretization [30,38]. (Recall u may be φ or ϕ while $u_0 = \phi_0$.)

It would seem to be the case that the subcell resolution (SR) technique is not required in order to achieve second-order accuracy with the Godunov Hamiltonian scheme. Without SR, the absolute error $||\nabla u| - g|$ does indeed scale as $O(h^2)$ (recall that g can be either 1 or f, see Sect. 3.2), but the interface location is generally not determined at the same level of accuracy, especially when the interface gradients of u and u_0 are different. This is particularly important for (5) because the information comes from the zero set of φ in (6). The interface gradient would be determined only with first order accuracy and the variation in the stretch function $D_s\chi(\Gamma(s))\hat{s}$ is then poorly captured. Thus, subcell resolution is still required to achieve second order accuracy for the Godunov Hamiltonian scheme. For example, when $u_{0,ij}u_{0,i-1,j} \leq 0$, we modify D_x^- for (x_i, y_j) to

$$D_x^- u_{ij} = \frac{u_{ij}}{\delta_{ij}^{x-}} + \frac{\delta_{ij}^{x-}}{2}\mathrm{minmod}(D_{xx}u_{i-1,j}, D_{xx}u_{ij}),$$

and D_x^+ for (x_{i-1}, y_j) is similarly modified. For time discretization we again use Gauss–Seidel iteration using the same spatially varying timestep as in (36).

The numerical Hamiltonian is monotone ([13]) and ensures the correct direction of information propagation. $u(x \in \Gamma, \tau) = 0$ is ensured by the numerical scheme. Recall that the proper viscosity solution given by (9) is introduced to ensure uniqueness on the unbounded domain, which is the desired level set function for our reinitialization. If the problem domain is a large ball B_n with Dirichlet boundary conditions, the proper viscosity solution in the unbounded domain is identical to the viscosity solution in $B_{n/3}$. The numerical solution obtained will not change in $B_{n/3}$ whether we solve it in the unbounded domain or in B_n since the equation is hyperbolic and we follow the characteristics. The convergence to the proper viscosity solution is equivalent to the convergence to the usual viscosity solution in the bounded domain. While not identical to the case of present interest, in [13] monotone schemes of $u_t + H(\nabla u) = 0$, where H is continuous, have been shown to converge to the viscosity solution. For our scheme, with the subcell resolution and Gauss–Seidel iteration, the proof is difficult but in practice we do observe the expected convergence.

5 Application to the Eulerian Immersed Boundary Method

As was previously mentioned, the LGPR procedure for reinitialization makes the local level set approach in the Eulerian immersed boundary method possible. The immersed boundary method was developed to study blood flow around heart valves in the 1970s [39] and has since been made more accurate [25,31,33]. At each timestep the immersed body is advected with the fluid velocity, and structural forces are spread back to the fluid through smoothed delta functions with compact support. Meanwhile, the Eulerian immersed boundary method [9–11] avoids the use of Lagrangian markers, which removes an instability when evolving the location of a stiff interface in explicit time-stepping schemes. It is also an effective method for avoiding "volume leakage" [10]. The tradeoff is that the computational cost is generally higher than Peskin's original method.

In a local level set approach (see [38]), the level set function is only retained in a small computational tube around the interface Γ, resulting in considerable computational savings when applied to the Eulerian immersed boundary method [10]. For relatively thin tubes and large interface deformations, however, the interface may approach the tube boundary and reinitialization may become necessary (such an example is included in Sect. 6). Previously, generic problems with spatially-varying tension around the interface could not be reinitialized without losing important stretching information, but by using the LGPR procedure, the local level set approach can be freely employed.

The algorithm is as follows. First, given the initial location of the immersed interface, $\Gamma(\xi)$, construct the signed distance function $\varphi(x)$. Then at each time step the following steps are performed:

1. Let $T = \{x : |\varphi(x)| < \gamma\}$ be the thin computational tube surrounding Γ, where γ is some positive constant. Store a cutoff function (see [38]), $\psi_T(x) = c(\varphi(x))$, where

$$c(y) = \begin{cases} 1 & |y| \le \beta, \\ (\gamma-\beta)^{-3}(|y|-\gamma)^2(2|y|+\gamma-3\beta) & \beta < |y| \le \gamma, \\ 0 & |y| > \gamma, \end{cases}$$

   for some constant $\beta < \gamma$. If the desired level set function ϕ has not yet been initialized, set $\chi(x \in \Gamma) = |X_\xi|$ and use the LGPR method to obtain ϕ in T (details are included below). Otherwise, reinitialize ϕ using LGPR as discussed in the previous sections.

2. Solve the equations of motion for the fluid–structure interaction problem, where the fluid force at the interface is given by (1). Evolve ϕ inside T with $\psi_T(x)u$ used to convect the level set function, where u is the velocity field.
3. If the interface remains far enough from the boundary of the computational tube and if $|\nabla\phi|_\Gamma \in [1-c, 1+c]$ for a chosen c, skip to Step 2 in the following timestep. Otherwise, let T_0 be the $(\beta-\alpha)$ neighborhood of T, for some constant $\alpha < \beta$, reinitialize the level set function to the signed distance function in T_0, and continue to Step 1 in the following timestep.

In Step 1, the LGPR method can be used to initialize the level set function ϕ. In a thin tube containing the interface, for every grid point (x_i, y_j), writing $z = P(x_i, y_j) = X(\xi_z)$ as the projection onto Γ, we determine the distance by computing $d = |(x_i, y_j) - z|$ and the sign of of the signed distance function φ by checking $((x_i, y_j) - z) \times X_\xi(\xi_z)$. We record $|X_\xi(\xi_z)|$ at the point (x_i, y_j), which is the value of $|\nabla\phi_{0,ij}|$. The distance function $d(x)$ is obtained by the fast sweeping method [52] and the sign is extended in a similar manner. φ

is then determined, and (5) is evolved to improve φ. The values of the cost function f at the interface are interpolated from $|\nabla\phi_{0,ij}|$. LGPR is then applied to recover ϕ.

The LGPR method is independent of the fluid model and makes possible the local level set approach to solving a broad range of interesting fluid–structure interaction problems beyond classical Newtonian flows; immersed boundary techniques have been used to study the interaction of deformable bodies with viscoelastic fluids related to peristaltic pumping [48], vesicles in nematic liquid crystals [32], and cell deformation [4], blebbing [46] and locomotion [7,8,17,49,50].

6 Numerical Experiments

In this section we implement and test the LGPR method using a few illustrative examples. In the first example we show how the LGPR method can be used to initialize level set functions from a given parametric curve. In Example 2, we show that the method achieves the expected accuracy in a setting in which the initial level set function and interface stretching are specified, and we show that the elastic force is preserved through the reinitialization process. Finally, in Example 3 we simulate the behavior of a relaxing, initially stretched membrane in a fluid using a local level set approach to the Eulerian immersed boundary method, and show that reinitialization is necessary and effective when the membrane approaches the boundary of the computational tube.

6.1 Example 1: Initializing a Level Set Function

The LGPR method may be used to initialize the level set function from a given parametric curve. Consider the ellipse given by $X(\xi) = (2\cos(\xi), \sin(\xi))$, where $0 \le \xi < 2\pi$ and ξ is the arc-length. Using the method as described in Sect. 5 results in a level set function which satisfies the desired property that $|\nabla\phi|(X(\xi)) = |X_\xi(\xi)|$. Figure 1 shows the numerical results on the domain $[-2.5, 2.5]^2$ with spatial grid size $h = 5/128$. The characteristic lines intersect on the medial axis of the ellipse and our extension scheme gives good results at the medial axis. The interface is well captured by our constructed level set function (Fig. 1c). To test the accuracy of the location and the interface gradient, we plot in Fig. 2 the location error $\mathcal{E}_L = \max_p\{|x_p^2/4 + y_p^2 - 1|\}$ and the gradient error $\mathcal{E}_G = \max_p\{||\nabla\phi|(p) - \sqrt{4y_p^2 + x_p^2/4}|\}$, where p is a point on the interface, $p = (x_i, y_\Gamma)$ or $p = (x_\Gamma, y_j)$. The interface location is retained with roughly third order accuracy while the interface gradient is retained with second order accuracy, as desired.

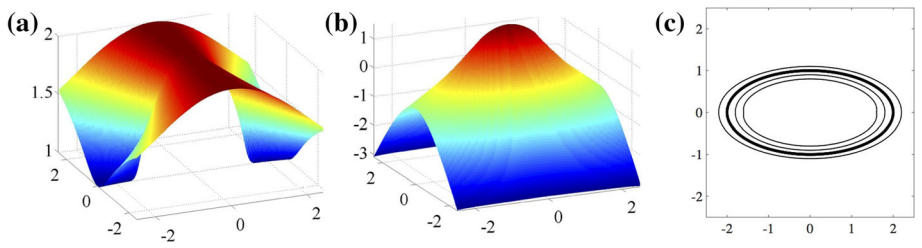

Fig. 1 Initialization of a level set function. **a** The cost function constructed from the parameterized interface $X(\xi) = (2\cos(\xi), \sin(\xi))$, where $0 \le \xi < 2\pi$. **b** The constructed level set function. **c** Contours of the level set function; the *bold line* is the specified interface

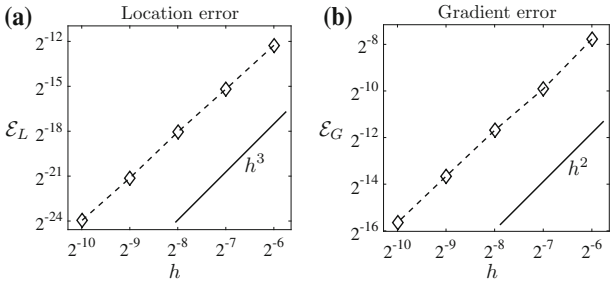

Fig. 2 **a** The results of numerical simulations are shown as *symbols*. The interface location error for the constructed level set function in Example 1 decays as $O(h^3)$. **b** The interface gradient error for the constructed level set function decays as $O(h^2)$

6.2 Example 2: Accuracy of Numerical LGPR

We now present a typical example in which the cost function is discontinuous in order to show that the transport equation is successfully solved and that the interface gradient is preserved with the desired accuracy. Let the surface Γ be parameterized in polar coordinates by $r(\theta) = 1 + 0.25\cos(3\theta)$. We take as the initial level set function $\phi_0(x, y) = \varphi(x, y)\exp(0.5y)$ where φ is the signed distance function relative to Γ. Since the interface is non-convex, characteristics of φ from the interface intersect both inside and outside of Γ.

Using the computational domain $[-1.5, 1.5]^2$ and grid size $h = 3/256$, we show in Fig. 3a, b two views of the cost function f produced by solving the transport equation. The set where f is discontinuous (the cut locus, where characteristics intersect) is well captured. The cost function does not oscillate near the cut locus using our scheme for solving the transport equation. Figure 3c, d show the numerical solution of the reinitialized level set function ϕ and its contours, which converges rapidly even though f is discontinuous.

To test the accuracy of the numerical method, we find all the interface points $p^0 = (x_\Gamma^0, y_j)$ or $p^0 = (x_i, y_\Gamma^0)$ by the interpolation formula (30) using the data ϕ_0 and correspondingly points $p = (x_\Gamma, y_j)$ or $p = (x_i, y_\Gamma)$ using ϕ. The gradients $\nabla\phi_0$ and $\nabla\phi$ are computed using (29) except that $\delta_{ij}^{x\pm}$ and $\delta_{ij}^{y\pm}$ are computed using the level set functions themselves instead of φ. We define the interface location error by $\mathcal{E}_L = \max\{|x_\Gamma^0 - x_\Gamma|, |y_\Gamma^0 - y_\Gamma|\}$, error in the interface gradient by $\mathcal{E}_G = \max\{|\nabla\phi_0(p^0) - \nabla\phi(p)|\}$ and the stretching error by $\mathcal{E}_S = \max\{||\nabla\phi(p)| - \exp(0.5y_p)|\}$. Fig. 4a–c show the decay rate of these errors with the spatial step size h. The error in the computed interface position decays roughly as $O(h^3)$, while $\nabla\phi$ (both the direction and norm) is accurate to $O(h^2)$ as expected. Elastic forces computed using the reinitialized level set function are therefore expected to carry over with first order accuracy, which we now probe.

Figure 5a, b show the x-component of the force associated with the prescribed stretching in the first example, before reinitialization using ϕ_0 (a) and after reinitialization using ϕ (b). For $y > 0$, $|\nabla\phi| > 1$ (the interface is in tension) while for $y < 0$, $|\nabla\phi| < 1$ (the interface is in compression). The force is computed on $[-1.5, 1.5]^2$ with $h = 3/128$, using a Hookean elastic energy $E(\chi) = (K/2)(\chi - 1)^2$ (with $K = 5$). Following Peskin [39], in the description of the force (1) that might be used in an immersed boundary context we use a smoothed δ function, $\delta_h = \mathbb{1}_{\{|\phi|\leq 3h\}}(1+\cos(\pi\phi/(3h)))/(6h)$. The traditional reinitialization method would naturally lose information about interface stretching, but here we see that the elastic force is preserved through the reinitialization process.

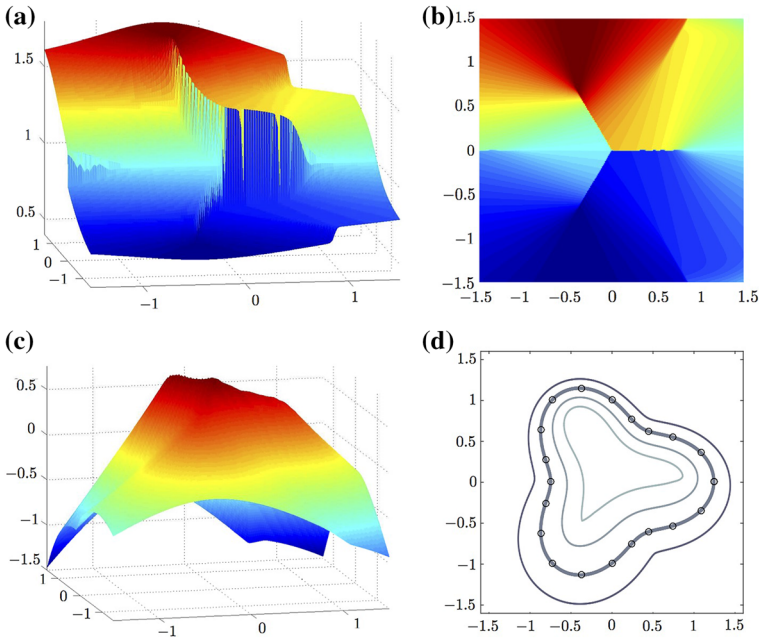

Fig. 3 Example 2. **a** The discontinuous cost function f constructed from the specified stretch $\chi = \exp(0.5y)$ on the interface $r(\theta) = 1+0.25\cos(3\theta)$. **b** The same as **a** from above. The cut locus (where f is discontinuous) is more readily apparent. **c** The level set function ϕ after reinitialization. **d** Contour plots of the level set function after reinitialization. The *bold line* is the zero set corresponding to Γ while *symbols* are sample positions on the interface computed analytically

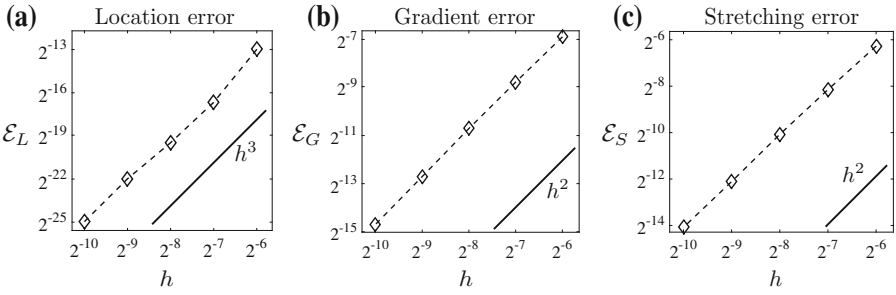

Fig. 4 Convergence results for Example 2, with computed values shown as *symbols*. **a** The error in the interface location decreases roughly as $O(h^3)$. **b** The error in the interface gradient decays as $O(h^2)$. **c** The error in the interface stretching computed using the reinitialized level set function decays as $O(h^2)$

We now test the accuracy in computing both the tangent gradient of the cost function and the stretching derivative (the tension gradient in the case of Hookean elastic energy). We define $Tf(p^0) = \nabla f \cdot (I - \hat{n}\hat{n})(p^0)$ where $\hat{n}(p^0) = \nabla\phi^0/|\nabla\phi^0|$ and correspondingly $T\chi(p^0) = \nabla \exp(0.5y)\cdot(I-\hat{n}\hat{n})(p^0)$. The cost function gradient error $\mathcal{E}_f = \max\{|Tf(p^0)-T\chi(p^0)|\}$ and the stretching derivative error $\mathcal{E}_{S'} = \max\{|\hat{n}\cdot\nabla\nabla\phi\cdot(I-\hat{n}\hat{n})(p)-\hat{n}\cdot\nabla\nabla\phi^0\cdot(I-\hat{n}\hat{n})(p^0)|\}$, where $\hat{n}(p) = \nabla\phi/|\nabla\phi|$ are then defined. The gradients (∇f, $\nabla\phi$ etc) are computed using (29), and $\nabla\nabla\phi(p)$ is computed by interpolating the corresponding Hessians at the two nearby points. As shown in Fig. 6, the quantities are computed with first order accuracy as expected.

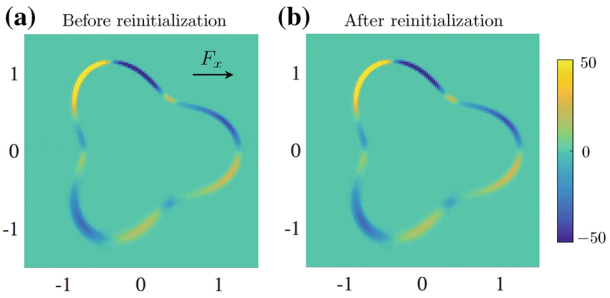

Fig. 5 The x-component of the elastic force F_x in Example 2 due to the complex initial stretching, using grid size $h = 3/128$, before reinitialization (**a**) and after reinitialization (**b**). The force computed has different relations with the curvature for $y > 0$ and $y < 0$. The traditional reinitialization method would naturally lose information about interface stretching, but here we see that the elastic force is preserved through the reinitialization process

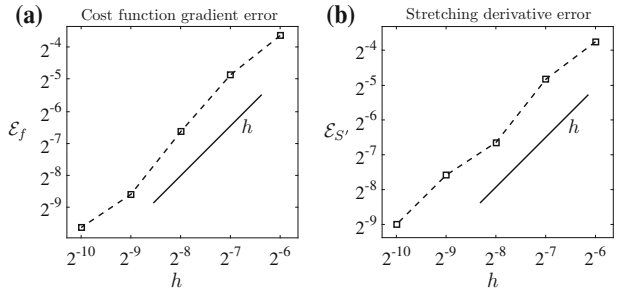

Fig. 6 **a** The error in the computed cost function gradient. **b** The error in the stretching derivative (the tension gradient in the case of Hookean elastic energy). Both are first order accurate as expected

6.3 Example 3: Eulerian Immersed Boundary Method with Local Level Sets

As a final example, we apply LGPR in the local level set approach to the Eulerian immersed boundary method. We simulate the dynamics of a relaxing membrane in a fluid in two-dimensions, where reinitialization becomes necessary as the interface approaches the tube boundary. The fluid is described by the Navier–Stokes equations,

$$\rho\,(u_t + u \cdot \nabla u) = -\nabla p + \mu \nabla^2 u + F, \tag{40}$$

$$\nabla \cdot u = 0, \tag{41}$$

where ρ is the fluid density, μ is the viscosity, u is the fluid velocity, and p is the pressure and F is the body force [3]. The equations represent conservation of momentum and mass, respectively. When scaled upon a characteristic length scale L, times scale T, velocity scale L/T and body force scale $\rho L/T^2$, the dimensionless equations read

$$u_t + u \cdot \nabla u + \nabla p = \frac{1}{Re}\nabla^2 u + F, \tag{42}$$

$$\nabla \cdot u = 0, \tag{43}$$

where $Re = \rho L^2/(\mu T)$ is the dimensionless Reynolds number, a measure of the relative importance of inertial to viscous effects. Fixing $Re = 1$, we solve the fluid equations above using the projection method of Kim and Moin [23] on a two-dimensional rectangular grid

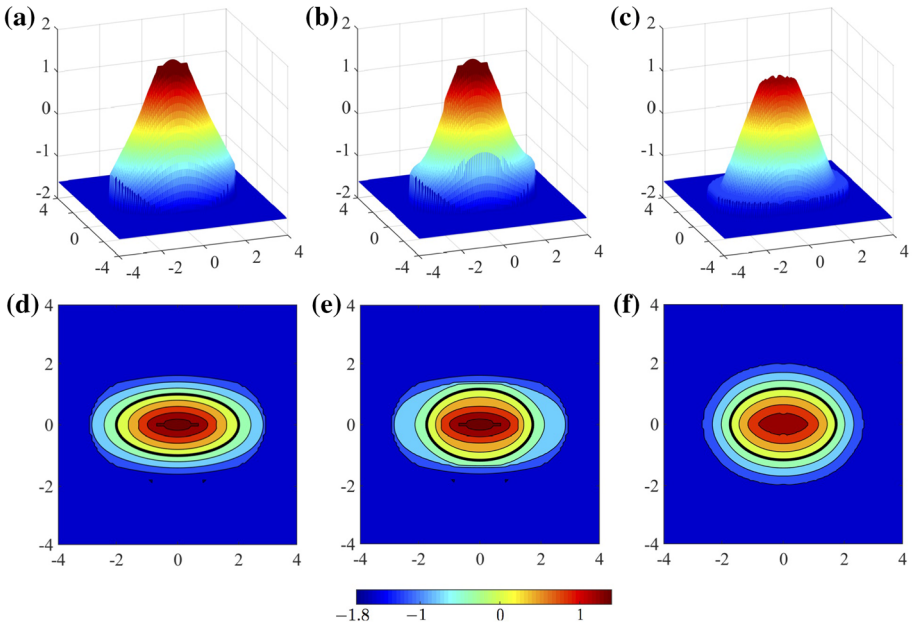

Fig. 7 Example 3. An initially stretched elastic membrane relaxes in a Navier–Stokes flow. The fluid–structure interaction is computed in a small region surrounding the membrane (a local level set method). **a**, **d** The initial level set function, and its contours, with the interface shows as a *dark black line*. **b**, **e** The level set function and contours after the membrane has partially relaxed; the membrane approaches the boundary of the computational tube containing the interface, leading to the development of errors. **c**, **f** The level set function after reinitialization; the interface is again well separated from the computational boundary, and the stretching information has been preserved

with no-slip boundary condition. The level set function is only constructed and updated in a tube that contains the interface. In its undeformed state the membrane has an arc length parameter ξ, where $0 \leq \xi < 2\pi$. To begin the simulation the membrane is initially stretched to an ellipse given by $X(\xi) = (2\cos(\xi), \sin(\xi))$, and the initialization of the level set function is exactly that performed as Example 1. The system evolves under the tension generated by the curve. The stretching energy is given again by linear elasticity, $E(\chi) = (K/2)(\chi - 1)^2$ with $K = 5$ and F is given by Eq. (1) with the same smeared delta functions as in Example 2.

We solve the equations above on the domain $[-4, 4]^2$ with uniform grid spacing $h = 8/100$. The tube and approachment warning parameters in the algorithm in Sect. 5 are chosen as $(\alpha, \beta, \gamma) = (4h, 8h, 10h)$. The system is evolved using a timestep of size $\Delta t = 0.3h$ (see [23]). In solving the sequence of reinitialization Eqs. (5)–(7), the CFL condition is satisfied by choosing $C = 0.5$ in (36). We set the number of iterations in pseudo-time a priori: specifically, we find the upper bounds for the pseudo-times needed [for (5) and (6) the bounds are γ, and for (7) the bound is $c_2\gamma/c_1$], and then set the number of iterations in each case to the bound divided by $0.5h$.

Figure 7a, d shows the initial level set function and its contours, with the interface shown as a dark black line. As the membrane relaxes over time, the level set function evolves to the one shown in Fig. 7b, e. The level set function is no longer adequate: the interface is close to the boundary of the tube where the local level set method is applied, and the level set function

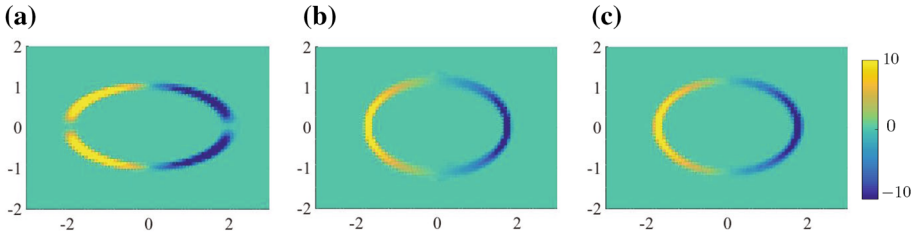

Fig. 8 The x-component of the force from Example 3. **a** The initial force distribution. **b** The force after partial relaxation but before level set reinitialization. **c** The force after reinitialization is preserved through the LGPR process

has a large gradient in the computational domain (though not yet at the interface). At this point we perform the LGPR algorithm in another tube that contains the new interface. The resulting level set is shown in Fig. 7c, f. The new level set function is better behaved and the sources of possible numerical error associated with the membrane approaching the boundary have vanished. The x-component of the force before and after reinitialization is shown in Fig. 8. The force is preserved with the expected error.

7 Conclusion

We have extended the traditional reinitialization process of a level set function to a locally gradient-preserving reinitialization method, which preserves not only the interface location, but also information about tangential interface stretching. We have shown that the proposed method can correctly yield a desired level set function. In particular, we have shown that the viscosity solution of the reinitialization equation converges to the unique "proper" viscosity solution of the eikonal equation, which is the desired level set function. Numerical schemes are proposed to solve these PDEs. The subcell resolution method for the transport equation is easy to implement and can extend the interface gradient to the whole domain with high accuracy. Numerical examples show that our method is successful, even for discontinuous cost functions. In applications, a local level set method is desirable for computational cost reductions, and the LGPR method can be applied in a small region containing the interface Γ. We showed that this reinitialization process makes the local level set approach to the Eulerian immersed boundary method possible in the general setting where fluid and elastic forces depend on interface stretching.

Acknowledgements X. Xu acknowledges support by NSF-DMS Grant 1159133.

Appendix A: Cut Locus of the Interface

We first show that the signed distance function φ is not differentiable at any point in A.

Lemma 3 *Under the assumptions stated in Sect. 3, φ is not differentiable at any point in A.*

Proof Since $\bar{A} \cap \Gamma = \emptyset$, to show that φ is not differentiable we show that $d(x, \Gamma)$ is not differentiable at $x \in A \cap U$ (the treatment of $A \cap U^c$ is similar). By the definition of A, we can find $y_1, y_2 \in \Gamma$, $y_1 \neq y_2$ so that $d(x, y_1) = d(x, y_2) = \varphi(x)$. Suppose that φ is

differentiable at x. We must have $|\nabla\varphi(x)| = 1$. Let $\hat{n} = \nabla\varphi(x)$. We have $x + \varepsilon\hat{n} \in U$ for small enough $\varepsilon > 0$. The inequality $d(x + \varepsilon\hat{n}, y_1) \geq \varphi(x + \varepsilon\hat{n}) > \varphi(x)$ then gives

$$d(x + \varepsilon\hat{n}, y_1) - d(x, y_1) \geq \varepsilon + o(\varepsilon), \tag{44}$$

and the law of cosines tells us that $\angle(\hat{n}, x - y_1) = 0$. But the same argument indicates that $\angle(\hat{n}, x - y_2) = 0$, leading to a contradiction.

We now show that if U is convex, $d(\bar{A}, \Gamma) = d(A, \Gamma) \geq \inf\{1/\kappa\} > 0$. This follows from the following lemma about the local structure of the curve satisfying Assumption 1.

Lemma 4 *For any $a \in A$ and any two points $y, z \in P(a)$, if the portion of Γ between y and z is the graph of a function over the segment yz, then $\exists\, w$ on the portion such that $\kappa(w)\mu(a) \geq 1/d(a, \Gamma)$ where $\mu(a) = 1$ if a is inside Γ and $\mu(a) = -1$ otherwise.*

Proof We take the straight line yz to be the x_1-axis, and assume at point z that the tangent line of Γ has a positive slope with angle θ. The projections of y and z to the x_1-axis are denoted by y_1 and z_1. As the portion of Γ between y and z is the graph of a function of x_1, then so is κ: $\kappa = \kappa(x_1)$. By integrating κ between y_1 and z_1 (κ is integrable by the assumption on the interface), we have

$$\mu(a) \int_{y_1}^{z_1} \kappa(x_1) dx_1 = 2\sin(\theta). \tag{45}$$

By basic trigonometry, $z_1 - y_1 = 2d(a, \Gamma)\sin(\theta)$. Hence, we can find $w_1 \in [y_1, z_1]$ so that

$$\mu(a)\kappa(w_1) \geq \frac{2\sin(\theta)}{2d(a, \Gamma)\sin(\theta)} = \frac{1}{d(a, \Gamma)}. \tag{46}$$

Returning to the previous claim, if U is convex, then $A \subset U$, $\mu(a) = 1$ and $\kappa(w) \geq 0$, and the claim then follows from Lemma 4.

Although we will not use the following "no cusp" property in this paper, this is still an interesting property of the cut locus geometry. This property is crucial in the literature when the uniqueness of the viscosity solution to the eikonal equation is discussed.

Theorem 4 *For a locally analytical boundary Γ, there are no cusps with zero angles in $\bar{A}$.*

Proof We will sketch the proof without details. Consider $\bar{A} \cap U$ as the example. Suppose that there are two edges making a zero angle at $x \in \bar{A} \cap U$. Parametrize them with arc lengths: $\gamma_1(s)$ and $\gamma_2(s)$, such that $\gamma_1(0) = \gamma_2(0) = x, \gamma_1'(0) = \gamma_2'(0) =: \hat{n}$ and that $\forall\varepsilon > 0$, $\exists s_\varepsilon \in (0, \varepsilon)$, $\gamma_1(s_\varepsilon) \neq \gamma_2(s_\varepsilon)$. By Lemma 1, there is an opening region between γ_1 and γ_2. Choose a sequence x_k approaching x inside the region such that the projection of Px_k (which is one point) approaches y. Then $y \in P(x)$. By Lemma 1, x_k-Px_k doesn't intersect with $\bar{A}$. As a limit line segment, x-y doesn't cross γ_1, γ_2 and thus is tangent to the two curves, namely $\hat{n} = (y - x)/|y - x|$. γ_1 and γ_2 must be on the two sides of the line xy. Consider γ_1 and the portion of Γ on that side, parametrized as $\Gamma_0(u)$ with $\Gamma_0(0) = y$. Then there exists a $\delta > 0$ such that the curvature is a smooth function on $[0, \delta]$ (if necessary, redefine $\kappa(0) = \lim_{u\to 0^+} \kappa(u)$). Choose $s_k \to 0^+$ such that $\#P\gamma_1(s_k) \geq 2$. From the fact that $x - y$ is the tangent line of γ_1 at x, $x - \gamma_1(s_k)$ and $\gamma_1(s_k) - y$ are almost parallel for sufficiently large k. Then, for k large enough, $w_k \in P\gamma_1(s_k)$, $d(x, w_k) \geq d(x, y)$ implies that w_k must fall onto $\Gamma_0(s)$ for $0 \leq s \leq \delta$. Using $\gamma_1(s_k) = x + s_k\hat{n} + O(s_k^2)$ and $P(x + s_k\hat{n}) = y$, we know $\forall w_k \in P\gamma_1(s_k)$ that $|w_k - y| = O(s_k^2)$. By Lemma 4 and since δ is small, there is a u_k such that $\Gamma_0(u_k)$ is between two points in $P\gamma_1(s_k)$ and $\kappa(u_k) \geq 1/d(\gamma_1(s_k), \Gamma)$. It is clear that $u_k = O(s_k^2)$. The contradiction is obtained by noticing that $\kappa(0) \leq 1/d(x, y)$ and $O(s_k^2) = |\kappa(u_k) - \kappa(0)| \geq |1/d(\gamma_1(s_k), \Gamma) - 1/d(x, y)| \geq Cs_k$ for some $C > 0$. □

Appendix B: Existence and Uniqueness of Solutions of the Eikonal Equation with a Discontinuous Cost Function

Here we prove the existence and uniqueness of the viscosity solution to (4) (Theorem 2). The proof of existence is standard, but the proof of uniqueness is not. There is one essential difference to the cases under consideration in [14,16,37,44,45]: here, the cut locus may have bifurcation points. This means that there can exist a point x in the singular set of the cost function such that for any disc B centered at x, B will be divided by the singular set into more than two parts. The arguments in references [14,16,37,44,45] then do not apply. Note that there is another subtle difference in our proof. Although from Theorem 4 we have that there are no cusps with zero angles in the singular set of the cost function, our proof does not rely on this fact.

Existence

We take $x \in U$ as an example case. We show that ϕ_M is a viscosity solution; a similar argument applies to ϕ_m. Recall that $0 < c_1 \le f \le c_2$ and that f^ε, f_ε are given in (14). We have the following relationships:

$$\begin{aligned} c_1 &\le \operatorname{essinf}\{f(y)|y \in B(x, \sqrt{(c_2 - c_1)\varepsilon})\} \le f_\varepsilon(x) \le f_*(x) \\ &\le f^*(x) \le f^\varepsilon(x) \le \operatorname{esssup}\{f(y)|y \in B(x, \sqrt{(c_2 - c_1)\varepsilon})\} \le c_2. \end{aligned} \tag{47}$$

f_ε increases to f_* while f^ε decreases to f^*, and $f^\varepsilon(f_\varepsilon)$ is continuous. The corresponding solution ϕ^ε is given as in (9). One then could verify the following dynamic programming principle: for $x \in U$ and $0 \le s_1 \le d(x, \Gamma)$,

$$\phi^\varepsilon(x) = \inf_{\gamma \in \mathscr{C}} \left\{ \int_0^{s_1} f^\varepsilon(\gamma(s))ds + \phi^\varepsilon(\gamma(s_1))|\gamma(0) = x \right\}. \tag{48}$$

The proof of this principle is omitted here. For similar arguments, one could refer to Chapter 10 of [15]. A direct conclusion from this principle is that

$$\begin{aligned} &0 \le \phi^\varepsilon \le c_2 d(x, \Gamma), \\ &|\phi^\varepsilon(x) - \phi^\varepsilon(y)| \le c_2|x - y|. \end{aligned} \tag{49}$$

By the Arzela–Ascoli theorem, since $\bar{U}$ is compact, there is a subsequence ϕ^{ε_k} that converges uniformly to $\bar{\phi}$.

Now suppose that $\bar{\phi} - \zeta$ has a local maximum at $x_0 \in U$. For small $\delta > 0$, $\bar{\phi} - \zeta - \delta|x - x_0|^2$ has a strict local maximum at x_0. There is a sequence of local maxima x_k for $\phi^{\varepsilon_k} - \zeta - \delta|x - x_0|^2$ that converges to x_0 by the uniform convergence of the function sequence. Fixing $K > 0$, for $k > K$, we have

$$|\nabla\zeta(x_k) + 2\delta(x_k - x_0)| \le f^{\varepsilon_k}(x_k) \le f^{\varepsilon_K}(x_k). \tag{50}$$

Letting $k \to \infty$, since f^{ε_K} is continuous, $|\nabla\zeta(x_0)| \le f^{\varepsilon_K}(x_0)$. Sending $K \to \infty$, we obtain $|\nabla\zeta(x_0)| \le f^*(x_0)$. For a local minimum at x_0, the argument is similar. Here, we just use the modified function $\bar{\phi} - \zeta + \delta|x - x_0|^2$ and the inequalities

$$|\nabla\zeta(x_k) - 2\delta(x_k - x_0)| \ge f^{\varepsilon_k}(x_k) \ge f_{\varepsilon_k}(x_k) \ge f_{\varepsilon_K}(x_k) \tag{51}$$

for $k > K$. Thus, $|\nabla\zeta(x_0)| \ge f_*(x_0)$ and $\bar{\phi}$ is a viscosity solution.

Now, fixing any $\delta > 0$, we can find $K > 0$ so that $\bar{\phi}(x) + \delta > \phi^{\varepsilon_k}(x)$ when $k > K$ for any $x \in U$. However, $\exists\, \gamma$ with $\gamma(0) = x$ such that $\phi^{\varepsilon_k} + \delta > \int_0^L f^\varepsilon(\gamma(s))ds \ge \int_0^L f^*(\gamma(s))ds$.

Note that $f^*(\gamma(\cdot))$ is the infimum of continuous functions and thus Lebesgue measurable on $[0, T]$. Meanwhile, $\bar{\phi}(x) - \delta \le \phi^{\varepsilon_k}(x) \le \int_0^L f^{\varepsilon_k}(\gamma(s))ds$ for k large enough and any $\gamma \in \mathscr{C}$ with $\gamma(0) = x$ and $\gamma(L) \in \Gamma$. Now fixing γ and taking $k \to \infty$, the dominant convergence theorem tells us that $\bar{\phi}(x) - \delta \le \int_0^L f^*(\gamma(s))ds$. Hence:

$$\bar{\phi}(x) = \inf_{\gamma \in \mathscr{C}} \left\{ \int_0^L f^*(\gamma(s))ds, \ \middle| \ \gamma(0) = x, \gamma(L) \in \Gamma \right\} = \phi_M(x). \tag{52}$$

The dynamic programming principle for ϕ_M still holds and ϕ_M is also bounded and Lipschitz continuous with the same constants.

Uniqueness

We again fix $x \in U$, and show that $\phi_m(x) = \phi_M(x)$. For any $\varepsilon > 0$, we can find $\gamma \in \mathscr{C}$ with $\gamma(0) = x$ and $\gamma(L) \in \Gamma$ so that $\int_0^L f_*(\gamma(s))ds < \phi_m(x) + \varepsilon$. γ has no self-intersection by the definition of $\mathscr{C}$.

By Lemma 2, except at finitely many points, all the points in $\bar{A}$ belong to some open locally analytical curves and have a projection with size 2. Noticing that γ is an injection, we pick a set E that covers the finite irregular points such that the total length of γ falling into E is less than ε/c_2, where c_2 is the upper bound of f^*. Then the remaining part $\bar{A} \setminus E$ has the following properties: it is the disjoint union of N curve portions e_n, $1 \le n \le N$; for any $x \in e_n$, we can find a ball $B(x, r_x)$ ($r_x > 0$) so that every point in $\bar{A} \cap B(x, r_x)$ has a projection of size 2 and $\bar{A} \cap B(x, r_x)$ is real analytic.

Step 1. We first show that the cost function f has limits on both sides of the edge e_n.

For any $x \in e_n$, $B(x, r_x)$ is divided into two subdomains B_1 and B_2 by $\bar{A}$. Let $x_k \in B_1 \cap U$, $x_k \to x$. The sequence $w_k = Px_k$ has a limit point $z \in Px$. Further inspection reveals that z is the only limit point of w_k since $\#Px = 2$ and the sequences in B_2 give another. This means that for every sequence in B_1 converging to x, the projections converge to z. Hence, $\lim_{y \to x, y \in B_1} f(y) = \chi(z)$. If the limit function is f_1, by the continuity of projection on one side, f_1 is continuous on e_n. f_2 may be similarly defined.

Step 2. We now decompose $\bar{A}$ into several parts so that on each part $\int (f^* - f_*)(\gamma(s))ds$ can be dealt with appropriately.

Let e_n be equipped with the 1D Lebesgue measure m induced by the arc length, and let $F_n = \{x \in e_n : f_1(x) = f_2(x)\}$. Clearly, $f^* = f_*$ on F_n and F_n is closed. The set $e_n \setminus F_n = \{x \in e_n : f_1 - f_2 > 0, \text{ or } f_1 - f_2 < 0\}$ is open, thus is the disjoint union of countable subintervals in e_n. Since the sum of lengths of these subintervals is finite, we can find finitely many of them, say M_n of them, such that the measure of the remaining is small. For these M_n intervals, we can cover the endpoints and get M_n new subintervals denoted as I_i, $1 \le i \le M_n$. Hence, we can decompose e_n into G_n with $m(G_n) < \varepsilon/Nc_2$, F_n and $\cup_{i=1}^{M_n} I_i$. Let's consider all the $M = \sum_n M_n$ subintervals. $\exists \delta_1, \delta > 0$ that depend on E, F_n, G_n, $1 \le n \le N$, such that each subinterval I_i satisfies: $U_i = \{x : d(x, I_i) \le \delta_1\}$ is divided into two domains V_{i1}, V_{i2}, $f^* \in C(\bar{V}_{i2})$, $f_* \in C(\bar{V}_{i1})$, and $\inf_{x \in V_{i2}, y \in V_{i1}} f^*(x) - f_*(y) \ge \delta$. We have thus decomposed $\bar{A}$ into the union of following sets: $M = \sum_n M_n$ subintervals; a closed set on which $f_* = f^*$; and a set (union of G_n and E) with measure less than $2\varepsilon/c_2$.

Let $C_i = \{s : \gamma(s) \in I_i\}$ be a subset of $[0, L]$ and $C = \cup_{i=1}^{M} C_i$. It is clear that $\int_{[0,L] \setminus C} (f^* - f_*)(\gamma(s))ds < 2\varepsilon$. Hence, we only need to study the integral on C_i.

Step 3. We now obtain a local property of the portion of γ on C_i.

By the local smoothness of the edges, $\exists \alpha > 0$, $\delta_3 < \delta_1/2$, such that if $s_1, s_2 \in C_i$, with $s_2 - s_1 \le \delta_3$, then the length of I_i between $\gamma(s_1)$ and $\gamma(s_2)$ is at most $(s_2 - s_1) + \alpha(s_2 - s_1)^2$. If $\exists s \in (s_1, s_2)$ so that $\gamma(s) \notin \bar{V}_{i1}$, then there is an subinterval $[s_3, s_4] \subset [s_1, s_2]$ such that $s \in [s_3, s_4]$ and $\gamma((s_3, s_4)) \cap \bar{V}_{i1} = \emptyset$. Since $\delta_3 < \delta_1/2$, $\gamma([s_3, s_4])$ cannot leave $\bar{V}_{i2}$. Noticing that $f^* = f = f_*$ on $\gamma((s_3, s_4))$,

$$\int_{\gamma[s_3,s_4]} f_* ds = \int_{\gamma[s_3,s_4]} f^* ds > \int_J f_* ds + (s_4 - s_3)\delta - \alpha(s_4 - s_3)^2 c_2,$$

where J is the part of I_i between $\gamma(s_3)$ and $\gamma(s_4)$. If we pick δ_3 small enough, we could have $(s_4 - s_3)\delta - \alpha(s_4 - s_3)^2 c_2 > 0$. We replace $\gamma([s_3, s_4])$ with J and get a new curve $\tilde{\gamma}$, and we see that $\int_{\tilde{\gamma}} f_* ds < \int_\gamma f_* ds$. $\tilde{\gamma}$ may be self-intersecting. We can modify it as following: If J intersects with $\gamma(0, s_3)$. we find the infimum of $s_{\min}$ on $[0, s_3]$ so that $\gamma(s_{\min}) \in J$. Then we piece $\gamma[0, s_{\min}]$ and the part of J starting from $\gamma(s_{\min})$ together. Then, by the same method we can deal with the case when J intersects with $\gamma((s_4, L))$. Such s_3, s_4 pairs correspond to disjoint open intervals, so we can do this modification at most countable many times and get another curve $\gamma_1 \in \mathscr{C}$, so that $\int_{\gamma_1} f_* ds < \int_\gamma f_* ds$. Hence, without loss of generality we can assume γ satisfies this property: if $s_1, s_2 \in C_i$, $|s_2 - s_1| < \delta_3$, then $\gamma([s_1, s_2]) \subset \bar{V}_{i1}$.

Step 4. With the property obtained, we perturb the curve defined on C_i so that the integral on C_i can be treated.

C_i is closed and consists of countable closed intervals (they are subintervals of $[0, L]$, different from the intervals on the edge portion) and a nowhere dense set G_i' (G_i' may have positive measure). Moreover $G_i = \bar{G}_i'$ is still nowhere dense since the extra possible points are the endpoints of the intervals. By the assumption above, we may write $G_i = \cup_{j=1}^{N_1} G_{ij}$ for some $N_1 \in \mathbb{N}$. $[\inf G_{ij}, \sup G_{ij}] \setminus G_{ij}$ does not contain any interval of length $\ge \delta_3$ for any j, so that $\gamma([\inf G_{ij}, \sup G_{ij}]) \subset \bar{V}_{i1}$, and

$$\inf_{v_1 \in G_{ij_1}, v_2 \in G_{ij_2}} |v_1 - v_2| \ge \delta_3$$

Now, assume K is G_{ij} or one of the intervals in C_i, and let $s_l = \inf K$, $s_r = \sup K$ and $\varepsilon_1 > 0$ be fixed. We can find finitely many points s_k in K and the difference between two consecutive points is less than δ_3. We shift $\gamma([s_k, s_{k+1}])$ along the normal of I_i at $\gamma(s_k)$ toward V_{i1} with distance δ_4. Now, we add line segments to connect the endpoints. The shifted curve portions and line segments are all in V_{i1} if δ_4 is small enough. Denote the curve so obtained by γ'. By the uniform continuity of f_* in $\bar{V}_{i1}$, we have $\int_{\gamma'} f_* ds < \int_\gamma f_* ds + \varepsilon_1$. However, γ' may be self-intersecting. We now modify it following an essentially similar procedure as before: γ' consists of $\gamma[0, s_l]$, $\gamma[s_r, L]$ and the shifted curves together with line segments, denoted as $\tilde{P}$. Consider the first shifted curve portion with the line segment $\tilde{P}_1$. Suppose $k \ge 2$ is the largest number such that $\tilde{P}_k$ intersects with $\tilde{P}_1$. We find the first point on $\tilde{P}_1$ that is on $\tilde{P}_k$, then discard the part on $\tilde{P}_1$ after this point and all curve portions $\tilde{P}_l$ with $1 < l < k$ and the part on $\tilde{P}_k$ that is before this point. Since the portions are finite, this process can be terminated, resulting in $P \subset \tilde{P}$, $P \in \mathscr{C}$ that connects $\gamma(s_l)$ and $\gamma(s_r)$. The remaining work is the same as how J was modified before. Then, we find a new curve γ_2. $\int_{\gamma_2} f_* ds \le \int_{\gamma'} f_* ds$. By the construction, we have removed $K \setminus \{s_l, s_r\}$ from C_i without adding new points. Such sets are countable, we can finish this process and obtain a curve γ_3, so that $C_i(\gamma_3)$ consists of countably many points and $\int_{\gamma_3} f_* ds - \int_\gamma f_* ds < \varepsilon/M$ since ε_1 is arbitrary.

Hence, we are able to construct a curve γ_4 with $\gamma_4(0) = x$ and $\gamma_4(L) \in \Gamma$ (since it has the same endpoints as γ) such that $\int_{\gamma_4} f^* ds \leq \int_{\gamma_4} f_* ds + 2\varepsilon < \int_{\gamma} f_* ds + 3\varepsilon < \phi_m(x) + 4\varepsilon$, which verifies the condition so that $\phi_m(x) = \phi_M(x)$.

Appendix C: The Solution of the Reinitialization Equation

In this section we show that the formula given in (19) is a viscosity sub-solution of the level-set reinitialization equation. An argument showing that it is also a super-solution is similar.

Consider that $u - \zeta$, where ζ is C^∞, has a local maximum at (x_0, τ_0) for $\tau_0 > 0$. We show that the sub-solution condition is satisfied. If $\tau_0 > \tau_{x_0}$, then in a neighborhood of (x_0, τ_0), we have $\tau > \tau_x$ since τ_x is continuous on x. The solution does not depend on τ, and we also must have $\zeta_\tau(x_0, \tau_0) = 0$. The sub-solution condition is satisfied for $x_0 \notin \Gamma$ as the condition has already been verified for the eikonal equation. If $x_0 \in \Gamma$, $[\mathrm{sgn}(u_0)(|p| - g)]_*|_{p=\nabla\zeta(x_0), x=x_0} \leq 0$ is assured.

Consider $0 < \tau_0 \leq \tau_{x_0}$. Then $u_0(x_0) \neq 0$ since for any $x \in \Gamma$, we have $\tau_x = 0 < \tau_0$. Take $u_0(x_0) > 0$ (the result for $u_0(x_0) < 0$ is similar). Let $h_1 = \min\{\tau_0, d(x_0, \Gamma)\} > 0$. There exists $0 < h_2 \leq h_1$, such that the dynamical programming principle holds for $h < h_2$:

$$u(x_0, \tau_0) = \inf_{\gamma} \left\{ u(\gamma(h), \tau_0 - h) + \int_0^h g(\gamma(s)) ds \,\middle|\, \gamma(0) = x_0 \right\}. \tag{53}$$

We now show this principle. Since $\tau_0 \leq \tau_{x_0}$, for any $\varepsilon > 0$, we can find γ with $\gamma(0) = x_0$ such that $u(x_0, \tau_0) + \varepsilon > u_0(\gamma(\tau_0)) + \int_0^{\tau_0} g(\gamma(s)) ds$. By the definition, $\int_h^{\tau_0} g(\gamma(s)) ds + u_0(\gamma(\tau_0)) \geq u(\gamma(h), \tau_0 - h)$ whether or not $\tau_0 - h > \tau_{\gamma(h)}$. '$\geq$' is thus shown.

We now show the other direction. Let $B = \inf_\gamma \{\int_0^L g(\gamma(s)) ds | \gamma(0) = x_0, \gamma(L) \in \Gamma\}$, and fix an arbitrary $\gamma \in \mathscr{C}$, $\gamma(0) = x_0$. We will discuss both cases where either $\tau_0 < \tau_{x_0}$ or not.

Consider $\tau_0 < \tau_{x_0}$. Take $h_2 \leq h_1$ small enough so that $|x - x_0| < h_2, |\tau - \tau_0| < h_2$ implies $\tau < \tau_x$ due to the continuity of τ_x. Let $h < h_2$. We can find $\gamma_1, \gamma_1(0) = \gamma(h)$ such that $u(\gamma(h), \tau_0 - h) + \varepsilon > \int_0^{\tau_0 - h} g(\gamma_1(s)) ds + |u_0|(\gamma_1(\tau_0 - h))$ since $\tau_{\gamma(h)} > \tau_0 - h$. Connecting $\gamma(s) : 0 \leq s \leq h$ and γ_1, we find γ_2. $\gamma_2(\tau_0) = \gamma_1(\tau_0 - h)$. Then, $u(x_0, \tau_0) \leq \int_0^{\tau_0} g(\gamma_2(s)) ds + |u_0(\gamma_2(\tau_0))| < \int_0^h g(\gamma(h)) + u(\gamma(h), \tau_0 - h) + \varepsilon$.

We now assume that $\tau_0 = \tau_{x_0}$ (recall that we are discussing the case where $\tau_0 \leq \tau_{x_0}$). We must have that $u(x_0, \tau_0) = B$. Let $h < h_1$. If $\tau_0 - h \geq \tau_{\gamma(h)}$, then $\exists \gamma_1, \gamma_1(0) = \gamma(h)$, $\gamma_1(L) \in \Gamma$ where $L \leq \tau_0 - h$ such that $u(\gamma(h), \tau_0 - h) + \varepsilon > \int_0^L g(\gamma_1(s)) ds$. Then, connecting $\gamma(s) : 0 \leq s \leq h$ and γ_1, we get a new curve γ_3 with total length $h + L \leq \tau_0$. We then have $u(x_0, \tau_0) = B \leq \int_0^{L+h} g(\gamma_3(s)) ds < \int_0^h g(\gamma(s)) ds + u(\gamma(h), \tau_0 - h) + \varepsilon$. If $\tau_0 - h < \tau_{\gamma(h)}$, we can find $\gamma_1, \gamma_1(0) = \gamma(h)$ such that $u(\gamma(h), \tau_0 - h) + \varepsilon > \int_0^{\tau_0 - h} g(\gamma_1(s)) ds + |u_0|(\gamma_1(\tau_0 - h))$. Connecting $\gamma(s) : 0 \leq s \leq h$ and γ_1, we get γ_2. Since $\tau_0 = \tau_{x_0}$, $B \leq \int_0^{\tau_0} g(\gamma_2(s)) ds + |u_0(\gamma_2(\tau_0))|$ by the definition of $u(x_0, \tau_0)$. The same argument as in the previous paragraph follows.

Combining what we have, the dynamic programming principle follows. With this principle the sub-solution condition is easily verified: since $u(x_0, \tau_0) - \zeta(x_0, \tau_0) \geq u(\gamma(h), \tau_0 - h) - \zeta(\gamma(h), \tau_0 - h)$, we see that

$$\zeta(x_0, \tau_0) \leq \inf_{\gamma} \left\{ \zeta(\gamma(h), \tau_0 - h) + \int_0^h g(\gamma(s)) ds \,\middle|\, \gamma(0) = x_0 \right\}, \tag{54}$$

which implies that

$$\zeta_\tau(x_0, \tau_0) + |\nabla \zeta|(x_0, \tau_0) \leq g(x_0). \tag{55}$$

References

1. Adalsteinsson, D., Sethian, J.A.: A fast level set method for propagating interfaces. J. Comput. Phys. **118**, 269–277 (1995)
2. Aujol, J.F., Aubert, G.: Signed distance functions and viscosity solutions of discontinuous Hamilton–Jacobi equations. Technical Report RR-4507, INRIA (2002)
3. Batchelor, G.K.: An Introduction to Fluid Dynamics. Cambridge University Press, Cambridge (2000)
4. Bottino, D.C.: Modeling viscoelastic networks and cell deformation in the context of the immersed boundary method. J. Comput. Phys. **147**, 86–113 (1998)
5. Chang, Y.C., Hou, T.Y., Merriman, B., Osher, S.: A level set formulation of Eulerian interface capturing methods for incompressible fluid flows. J. Comput. Phys. **124**, 449–464 (1996)
6. Choi, H.I., Choi, S.W., Moon, H.P.: Mathematical theory of medial axis transform. Pacific J. Math. **181**(1), 57–88 (1997)
7. Chrispell, J.C., Cortez, R., Khismatullin, D.B., Fauci, L.J.: Shape oscillations of a droplet in an Oldroyd-B fluid. Phys. D **240**(20), 1593–1601 (2011)
8. Chrispell, J.C., Fauci, L.J., Shelley, M.: An actuated elastic sheet interacting with passive and active structures in a viscoelastic fluid. Phys. Fluids. **25**(1), 013,103 (2013)
9. Cottet, G.H., Maitre, E.: A level-set formulation of immersed boundary methods for fluid–structure interaction problems. C. R. Acad. Sci. Paris **338**, 581–586 (2004)
10. Cottet, G.H., Maitre, E.: A level set method for fluid–structure interactions with immersed surfaces. Math. Models Methods Appl. Sci. **16**, 415–438 (2006)
11. Cottet, G.H., Maitre, E.: Eulerian formulation and level set models for incompressible fluid–structure interaction. Math. Model Numer. Anal. **42**, 471–492 (2008)
12. Crandall, M.G., Lions, P.: Viscosity solutions of Hamilton–Jacobi equations. Trans. Am. Math. Soc. **277**, 1–42 (1983)
13. Crandall, M.G., Lions, P.: Two approximations of solutions of Hamilton–Jacobi equations. Math. Comput. **43**, 1–19 (1984)
14. Deckelnick, K., Elliott, C.M.: Uniqueness and error analysis for Hamilton–Jacobi equations with discontinuities. Interfaces Free Bound **6**, 329–349 (2004)
15. Evans, L.C.: Partial Differential Equations, 2nd edn. American Mathematical Society, Providence, RI (2010)
16. Festa, A., Falcone, M.: An approximation scheme for an eikonal equation with discontinuous coefficient. SIAM J. Numer. Anal. **52**(1), 236–257 (2014)
17. Guy, R.D., Thomases, B.: Computational challenges for simulating strongly elastic flows in biology. In: Spagnolie, S.E. (ed.) Complex Fluids in Biological Systems, pp. 359–397. Springer, New York (2015)
18. Harten, A.: ENO schemes with subcell resolution. J. Comput. Phys. **83**, 148–184 (1989)
19. Ishii, H.: Hamilton–Jacobi equations with discontinuous Hamiltonians on arbitrary open sets. Bull. Fac. Sci. Eng. Chuo Univ. **28**, 33–77 (1985)
20. Ishii, H.: Existence and uniqueness of solutions of Hamilton–Jacobi equations. Funkc. Ekvacio **29**, 167–188 (1986)
21. Ishii, H.: A simple, direct proof of uniqueness for solutions of the Hamilton–Jacobi equations of Eikonal type. Proc. Am. Math. Soc. **100**, 247–251 (1987)
22. Jin, S., Liu, H.L., Osher, S., Tsai, R.: Computing multi-valued physical observables for the high frequency limit of symmetric hyperbolic systems. J. Comput. Phys. **210**, 497–518 (2005)
23. Kim, J., Moin, P.: Application of a fractional-step method to incompressible Navier–Stokes equations. J. Comput. Phys. **59**(2), 308–323 (1985)
24. Koike, S.: A Beginner's Guide to the Theory of Viscosity Solutions. Mathematical Society of Japan, Tokyo (2004)
25. Lai, M.C., Peskin, C.S.: An immersed boundary method with formal second-order accuracy and reduced numerical viscosity. J. Comput. Phys. **160**, 705–719 (2000)
26. Li, Z., Zhao, H., Gao, H.: A numerical study of electro-migration voiding by evolving level set functions on a fixed Cartesian grid. J. Comput. Phys. **201**, 281–304 (1999)
27. Lieutier, A.: Any open bounded subset of R^n has the same homotopy type as its medial axis. Comput. Aided Des. **36**(11), 1029–1046 (2004)

28. Lions, P.L.: Generalized Solutions of Hamilton–Jacobi Equations. Cambridge University Press, Cambridge (1992)
29. Malladi, R., Sethian, J.A.: Image processing via level set curvature flow. Proc. Natl. Acad. Sci. **92**, 7046–7050 (1995)
30. Min, C.: On reinitializing level set functions. J. Comput. Phys. **229**, 2764–2772 (2010)
31. Mori, Y., Peskin, C.S.: Implicit second-order immersed boundary methods with boundary mass. Comput. Methods Appl. Mech. Eng. **197**, 2049–2067 (2008)
32. Mushenheim, P.C., Pendery, J.S., Weibel, D.B., Spagnolie, S.E., Abbott, N.L.: Straining soft colloids in aqueous nematic liquid crystals. Proc. Natl. Acad. Sci. **113**, 5564–5569 (2016)
33. Newren, E.P., Fogelson, A.L., Guy, R.D., Kirby, R.M.: Unconditionally stable discretizations of the immersed boundary equations. J. Comput. Phys. **222**, 702–719 (2007)
34. Osher, S., Fedkiw, R.: Level set methods: an overview and some recent results. J. Comput. Phys. **169**, 463–502 (2001)
35. Osher, S., Sethian, J.: Fronts propagating with curvature dependent speed: algorithms based on Hamilton–Jacobi formulations. J. Comput. Phys. **79**, 12–49 (1988)
36. Osher, S., Shu, C.: Higher-order essentially nonoscillatory schemes for Hamilton–Jacobi equations. SIAM J. Numer. Anal. **28**, 907–922 (1991)
37. Ostrov, D.N.: Extending viscosity solutions to Eikonal equations with discontinuous spatial dependence. Nonlinear Anal. **42**, 709–736 (2000)
38. Peng, D., Merriman, B., Osher, S., Zhao, H., Kang, M.: A PDE-based fast local level set method. J. Comput. Phys. **155**, 410–438 (1999)
39. Peskin, C.S.: The immersed boundary method. Acta Numer. **11**, 479–517 (2002)
40. Salac, D., Miksis, M.: A level set projection model of lipid vesicles in general flows. J. Comput. Phys. **230**(22), 8192–8215 (2011)
41. Sethian, J.A.: A fast marching level set method for monotonically advancing fronts. Proc. Natl. Acad. Sci. **93**, 1591–1595 (1996)
42. Sethian, J.A.: Level Set Methods and Fast Marching Methods: Evolving Interfaces in Computational Geometry, Fluid Mechanics, Computer Vision, and Materials Science, vol. 3. Cambridge University Press, Cambridge (1999)
43. Soravia, P.: Optimal control with discontinuous running cost: Eikonal equation and shape-from-shading. In: Proceedings of 39th IEEE Conference on Decision and Control, 2000, vol 1, pp. 79–84. IEEE (2000)
44. Soravia, P.: Boundary value problems for Hamilton–Jacobi equations with discontinuous Lagrangian. Indiana Univ. Math. J. **51**, 451–476 (2002)
45. Soravia, P.: Degenerate Eikonal equations with discontinuous refraction index. ESAIM: COCV **12**, 216–230 (2006)
46. Strychalski, W., Copos, C.A., Lewis, O.L., Guy, R.D.: A poroelastic immersed boundary method with applications to cell biology. J. Comput. Phys. **282**, 77–97 (2015)
47. Sussman, M., Smereka, P., Osher, S.: A level set approach for computing solutions to incompressible two-phase flow. J. Comput. Phys. **114**, 146–159 (1994)
48. Teran, J., Fauci, L., Shelley, M.: Peristaltic pumping and irreversibility of a Stokesian viscoelastic fluid. Phys. Fluids **20**(073), 101 (2008)
49. Teran, J., Fauci, L., Shelley, M.: Viscoelastic fluid response can increase the speed and efficiency of a free swimmer. Phys. Rev. Lett. **104**(3), 038,101 (2010)
50. Thomases, B., Guy, R.D.: Mechanisms of elastic enhancement and hindrance for finite-length undulatory swimmers in viscoelastic fluids. Phys. Rev. Lett. **113**(9), 098,102 (2014)
51. Tsai, Y.H.R., Cheng, L.T., Osher, S., Zhao, H.K.: Fast sweeping algorithms for a class of Hamilton–Jacobi equations. SIAM J. Numer. Anal. **41**(2), 673–694 (2003)
52. Zhao, H.K.: A fast sweeping method for Eikonal equations. Math. Comput. **74**(250), 603–627 (2005)